

REPORT DOCUMENTATION PAGE		READ INSTRUCTIONS BEFORE COMPLETING FORM
1. REPORT NUMBER AVRADCOM TR 83-F-6	2. GOVT ACCESSION NO.	3. RECIPIENT'S CATALOG NUMBER
4. TITLE (and Subtitle) QUALITY CONTROL AND NONDESTRUCTIVE EVALUATION TECHNIQUES FOR COMPOSITES - PART II: PHYSIO- CHEMICAL CHARACTERIZATION TECHNIQUES - A STATE- OF-THE-ART REVIEW		5. TYPE OF REPORT & PERIOD COVERED Final Report 8/5/82 to 4/4/83
7. AUTHOR(s) J. Koenig		6. PERFORMING ORG. REPORT NUMBER Monitoring Agency, TR 83-24
9. PERFORMING ORGANIZATION NAME AND ADDRESS Case Western Reserve University Cleveland, OH 44106		8. CONTRACT OR GRANT NUMBER(s) DAAG29-81-D-0100 TCN 82-214
11. CONTROLLING OFFICE NAME AND ADDRESS U.S. Army Aviation Research & Development Command ATTN: DRDAV-EGX 4300 Goodfellow Blvd., St. Louis, MO 63120		10. PROGRAM ELEMENT, PROJECT, TASK AREA & WORK UNIT NUMBERS D/A Project: 1827119 AMCMS Code: 1497.20 Agency Accession: DDS7119(EP2)
14. MONITORING AGENCY NAME & ADDRESS (if different from Controlling Office) Army Materials and Mechanics Research Center ATTN: DRXMR-K Watertown, Massachusetts 02172		12. REPORT DATE May 1983
		13. NUMBER OF PAGES 72
		15. SECURITY CLASS. (of this report) Unclassified
		15a. DECLASSIFICATION/DOWNGRADING SCHEDULE
16. DISTRIBUTION STATEMENT (of this Report) Approved for public release; distribution unlimited.		
17. DISTRIBUTION STATEMENT (of the abstract entered in Block 20, if different from Report)		
18. SUPPLEMENTARY NOTES		
19. KEY WORDS (Continue on reverse side if necessary and identify by block number) Composite materials Epoxy resins Curing Quality assurance Infrared spectroscopy State-of-the-art Quality control Fiber-reinforced composites		
20. ABSTRACT (Continue on reverse side if necessary and identify by block number) (SEE REVERSE SIDE)		

Block No. 20

ABSTRACT

The physical, chemical, and ultimate mechanical properties of high performance glass fiber-reinforced composites are dependent on the degree of cure and structure of epoxy matrices. Therefore, a knowledge of the curing process and composition of epoxy matrices is essential for relating the properties of composites to the extent of the reaction and optimizing the performance. Several methods have been developed to characterize and control the curing of epoxy matrices. These methods include spectroscopy, differential scanning calorimetry, dielectric analysis, and dynamical mechanical tests. These methods can be used to characterize the curing process during or after the fabrication of the cured epoxy matrices to justify reproducibility, reliability, and durability. In general, a combination of these methods are powerful techniques to analyze and control the quality of epoxy matrices in fiber-reinforced composites. The sensitivity, advantages, and selectivity of these techniques will be reviewed and discussed in this report.

AVRADCOM

Report No. TR 83-F-6

ADA131038

MANUFACTURING METHODS AND TECHNOLOGY
(MANTECH) PROGRAM

QUALITY CONTROL AND NONDESTRUCTIVE EVALUATION
TECHNIQUES FOR COMPOSITES - PART II: PHYSIOCHEMICAL
CHARACTERIZATION TECHNIQUES - A STATE-OF-THE-ART REVIEW

JACK L. KOENIG
Case Western Reserve University
Cleveland, Ohio 44106

May 1983

FINAL REPORT

Contract No. DAAG29-81-D-0100



Approved for public release;
distribution unlimited

U. S. ARMY AVIATION RESEARCH AND DEVELOPMENT COMMAND

PREFACE

This project was accomplished as part of the U.S. Army Aviation Research and Development Command Manufacturing Technology program. The primary objective of this program is to develop, on a timely basis, manufacturing processes, techniques, and equipment for use in production of Army material. Comments are solicited on the potential utilization of the information contained herein as applied to present and/or future production programs. Such comments should be sent to: U.S. Army Aviation Research and Development Command, ATTN: DRDAV-EGX, 4300 Goodfellow Blvd., St. Louis, MO 63120.

This work described in this report was accomplished under a contract monitored by the Army Materials and Mechanics Research Center. Technical monitor for this contract was Dr. R.J. Shuford.

1.0 INTRODUCTION

The physical, chemical, and ultimate mechanical properties of high performance glass fiber reinforced-composites are dependent on the degree of cure and structure of epoxy matrices. Therefore, a knowledge of curing process and composition of epoxy matrices is essential for relating the properties of composites to the extent of the reaction and optimizing the performance. Several methods have been developed to characterize and control the curing of epoxy matrices. These methods include spectroscopy, differential scanning calorimetry, dielectric analysis, and dynamical mechanical tests. These methods can be used to characterize the curing process during or after the fabrication of the cured epoxy matrices to justify reproducibility, reliability, and durability. In general, a combination of these methods are powerful techniques to analyze and control the quality of epoxy matrices in fiber-reinforced composites. The sensitivity, advantages, and selectivity of these techniques will be reviewed and discussed in this paper.

2.0 THE ROLE OF EPOXY MATRICES:

There are three major types of epoxy resins of commercial significance: (a) epichlorohydrin-bisphenol A (conventional), (b) epoxy novolak, and (c) epoxidized polyolefin resins(1). The most commonly used curing agents are anhydrides and amines. Miscellaneous modifications of epoxy systems are used to meet the specific performance requirements. In order to optimize the performance, several factors must be considered in choosing the epoxy resin for suitable composite matrices. These factors are based on the following considerations: (1) processing requirements (2) economic preference and (3) mechanical performance.

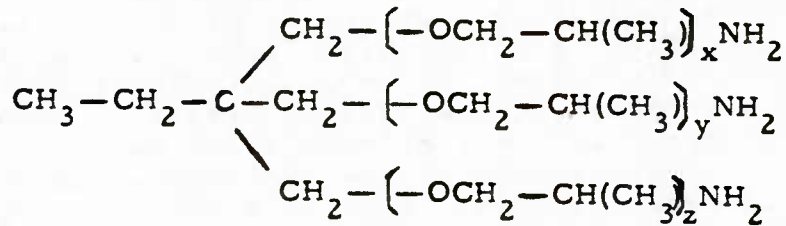
Processing requirements involve viscosity considerations (rheological behaviors of epoxy resins), high or low temperature cure, , etc. One of the ways of decreasing the viscosity of an epoxy resin is to add a diluent(2). Reactive diluents are liquid materials which have lower viscosity than the epoxy resin and are assimilated into the resin network during cure. Nonreactive diluents comprise materials which don't contain epoxide groups, but which are completely sorbed in the cured epoxy resin network. Nonreactive diluents may usually be removed by solvent extraction.

Since the inhomogeneities observed in cured epoxy resins by several workers appear to be related to the effectiveness of mixing the reactants, Tateosian and Royer(3) reported an improvement in impact strength by as much as 58% by use of dynamic mixing. J.P. Bell (4) studied the effect of mixing on homogeneity by using an electrical field to induce mixing of viscous fluids of different conductivity, and significantly increased the ultimate tensile strength of epoxy resins.

Another processing requirement is concerned with the temperature of cure. For advanced fiber composites, the difference in thermal expansion coefficients between the fiber and the epoxy matrices during the high-temperature-cure cycle creates a very serious problem such as visible delamination, or fiber microbuckling. On the other hand, the commonly used room temperature cured epoxy resins have some

disadvantages, such as poor mechanical properties and the working life is too short to be used in composite processing.

Moore(5) used a particular amine,



$$x+y+z=5.3$$

and pure diglycidyl ether of bisphenol A (DER 332 EPOXY) to fabricate polyether amine-cured epoxy matrices. In spite of good flexibility and toughness, this resin system has fairly well balanced mechanical properties. It can be room-temperature-cured and presents no problem in filament winding which requires a good epoxy resin of low viscosity and long working life.

For economic considerations, sometime it is necessary to consider energy savings as well as increases in productivity, then a fast-curing epoxy system is required. Cordova chemical(6) has developed accelerators that provide greater than a six fold advantage over tertiary amines in anhydride cured epoxies. It should be emphasized that the properties obtained with a short cure (2 hours) are the same as those properties previously requiring 12-24 hours for the curing process with the conventional accelerators. Generally the lower the temperature, the slower the reaction. On the other hand, the higher the temperature, the greater the risk of degradation. For production consideration, the optimum condition is the shortest cure time which will still assure a resin matrix with the desired properties.

A current problem with epoxy resin systems used in continuous fiber reinforced composites is their shelf-life. Once the resin is mixed, it must be used immediately or stored at low temperatures in the form of a prepreg. Prepregs must typically be stored at -18°C and, at this temperature, they are estimated to remain stable for six months. The ideal system from a storage point of view would be a prepreg which is stable at room temperature in the B-stage and which retains its tack and drape. Currently no such ideal system exists. However, a resin system which is cured with a sterically hindered amine is stable at room temperature in the B-stage in a glassy state. Upon mixing at room temperature, the primary amine hydrogens react to form a linear polymer. The secondary amine hydrogens do not react at room temperature because they are much less reactive due to the steric hindrance of the nearby methyl groups. The epoxy resin does not form a three-dimensional structure until the secondary amine hydrogens react upon additional heating. Buckley and Roylance(7) studied the curing kinetics of this system with FTIR. The shelf life at room temperature of the B-staged resin system is predicted to be at least three months based on an extrapolation of the experimental kinetic data.

On the other hand, the growing use of composite materials in commercial and military equipment has led to concern over field repair or patching of damaged composites. Field level repair has some unique materials requirements in terms of storage and curing characteristics. Since the presence of freezer storage space is not guaranteed, the resin used in the composite patch would necessarily require room-temperature stability. Also, since cure facilities are very limited, the resin system must be curable at low temperatures and times (150°C for one hour). Unfortunately, commercially available prepregs typically require both freezer storage and higher temperature cures. Donnellan and Roylance(8) used 2,5-dimethyl 2,5-hexane diamine as a hardener to form a linear glassy prepolymer at room temperature. The resin was found to react to a partially cured (52%) state at room temperature and then vitrify. Samples stored for a two-month period showed no advance to a more fully cured state. The isothermal curing behavior was studied in a temperature range from 100° to 150°C with FTIR.

Heat resistance is another requirement of the epoxy matrix. Several methods have been pursued to improve the Heat-Deflection-Temperature (thermal mechanical properties). Lauze(9) shows cured epoxy resins based on Bisphenol S have a considerable increase in heat resistance over those based on Bisphenol A. The increased heat resistance results from the replacement of the isopropylidene group in Bisphenol A with the more thermally stable sulfone group. The increased heat resistance results from the replacement of the isopropylidene group in bisphenol A with the more thermally stable sulfone group. The increased heat resistance is indicated by the resistance to heat aging, resistance to heat deformation as well as retention of strength at elevated temperature. The enhanced thermal properties of sulfone epoxy are achieved in a different way from that of the epoxy novolacs which results from an increase in the crosslinking density. Another way of improving the high temperature performance is to add a rigid structure in the backbone of epoxy resins. Polyimides have good high temperature performance and the epoxy resins possess many desirable properties of the aromatic polyimide if it contains the phthalimides moiety. Kaplan(10) has synthesized some of these epoxy/imide resins, and demonstrated good thermal stability. Another new family of resins is based on the glycidylated hydantoin ring(11). Because of the compact, polar heterocyclic structure of the hydantoin ring, the heat distortion temperature of these resins are significantly higher than comparably cured conventional epoxies. With aromatic rings replaced by heterocycles in the structure, smoke generation during combustion has been greatly reduced.

The primary role of epoxy matrices is to transfer stress from the fiber to the finished composites. Currently prevailing epoxy resins are designed for glass fiber in fabricating composites. Since graphite fibers have a higher modulus(5×10^7) than glass fiber(1×10^7 psi), it is important to use high strength matrices to maximize the efficient transfer of the fiber strength to the composites. Moller(12) synthesized a series of pure epoxy resins of the following structural types: diepoxy bisphenols, glycidyl esters, diepoxy cycloaliphatics, acyclic bisphenol, diepoxides and glycidyl amines, then correlated the mechanical properties to Bisphenol diepoxide structure. The glycidyl glycidate resins had a tensile strength of over 20000 psi; this is one of

the highest values ever reported for a bulk polymer. These kinds of resins can be used in the fabrication of high modulus graphite fiber reinforced composites. Another serious problem concerned with epoxy matrices in composite is the brittle nature of the fully cured resin. F. J. McGarry(13) has shown that the impact strength of aromatic epoxy resins can be improved by incorporating a specific carboxyl terminated elastomer in concentrations of up to 10 parts per hundred parts of resins. A. C. Soldatos(14) extended this investigation to cycloaliphatic epoxides, which have many outstanding properties, and got toughened epoxy resins without significantly degrading the heat distortion temperature. Liquid rubber can be used to toughen or flexibilize epoxy resins. The toughened epoxy resins show improved crack resistance and improved impact strength with a minimum loss of mechanical and thermal properties(heat distortion temperature). On the other hand, the flexibilized system are those where the liquid rubber has reacted with the epoxy resin and they are single phase systems. The flexibilized system provides epoxy matrices with high impact strength, but always accompanied with a significant loss in thermal-mechanical properties. The first criterion for a toughened system is that it should contain a dispersed second phase, and this phase must have a particle greater than about 1000 Å in diameter. The non-functional liquid rubber that contains no reactive groups to react with epoxy resins will have higher fracture energy and will not improve the impact strength. It(15) is generally accepted that three criteria are necessary for toughening : (1) proper size of dispersed phase (2) bonding between the matrices and the dispersed rubber (3) elastic character to the rubber particles. A. R. Siebert(15) showed that the toughest epoxy system are those where the second phase exists as a bimodal distribution of rubbery particles that contain small particles with 1000 Å diameters and large particles with 1-5 μ diameters. H. Samejima(16) reported a new elastomeric modified epoxy which gave a cured product having superior impact resistance. As shown in Figure 1, the thermal shock resistance is plotted versus the heat deflection temperature for polyetherester (PEE) modified epoxy resin, and epoxy resins blended with the flexible epoxy. It is obvious that flexible epoxy resins will decrease the HDT but improve the heat crack resistance value. On the other hand, the toughened epoxy resins improve the heat crack resistance value without sacrifice of HDT.

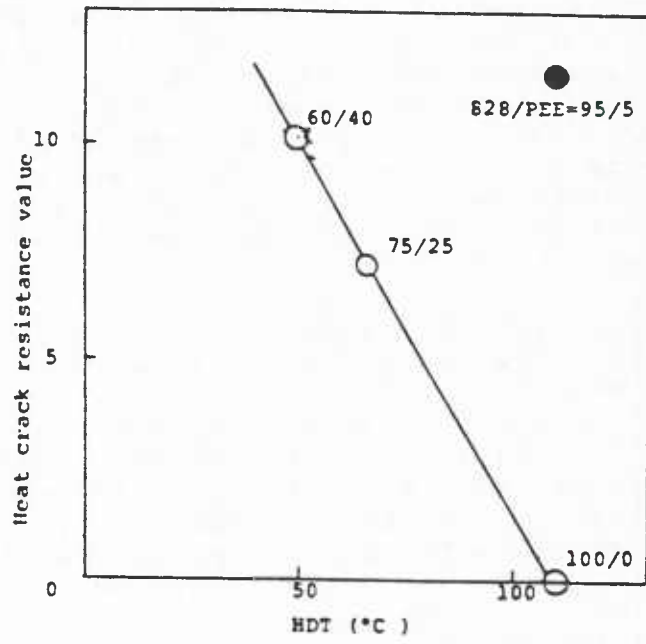


Figure 1. Heat distortion temprature vs. Thermal shock resistance value.

3.0 CALORIMETRIC ANALYSIS

The processing of epoxy resins, such as curing/crosslinking involves the exposure of these materials to various levels of heat treatment. The physical and mechanical performance and the quality of the cured articles are largely determined by the extent of cure, the control of temperature distribution, and the rate of temperature rise during processing. Moreover, temperature variations during cure, which determine the degree of cure in an epoxy resin system, depend to a large extent not only on the heat of the reaction but also on the specific heat and the thermal conductivity of the material at different stages of the cure cycle. These parameters can be characterized by DSC, and are essential for optimizing product quality and processing condition considering the heat transfer.

Differential Scanning Calorimetry, measures the difference in the rates of heat absorption or evolution, by a sample with respect to an inert reference as the temperature is raised at a constant rate. On the other hand, Differential Thermal Analysis (DTA) measures the differential temperature caused by heat changes in the sample. DSC can be used to characterize the curing reaction of epoxy resins in the presence of fillers or without it. The basic assumption made is that the heat of reaction is proportional to the extent of the reaction. Moreover, it is also assumed that the specific heat of the material either stays constant or varies linearly with scanning temperature during a scan while both the temperature and degree of cure change simultaneously. These assumptions are valid for simple reaction, but not obviously valid for the complicated crosslinking reactions which occur in the cure of epoxy resin. There are three ways (17) of measuring the extent of curing in epoxy resin. This can be achieved by (1) isothermal operation, (2) analysis of thermograms with different scan rates (3) scans on partly cured resins. For isothermal operation, because a short time is needed for the samples and the test cell to heat up to the desired temperature, the beginning portion of the exotherm is lost. Therefore, isothermal scans become unreliable for very fast cures. This problem can be solved by analysis of thermograms with different scan rates. Figure 2 shows a series of thermograms with different scan rates on a temperature axis.

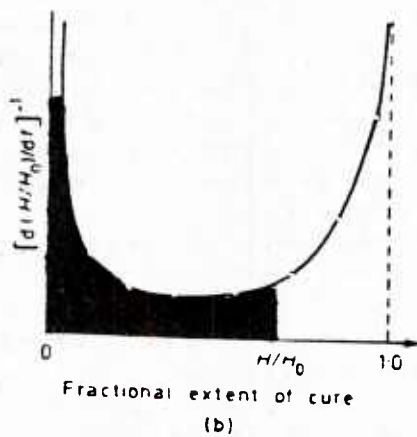
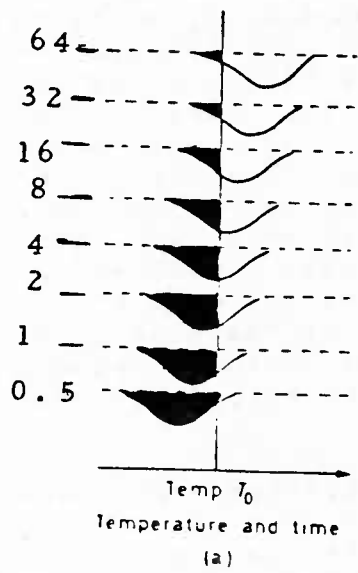


Figure 2. (a) Set of displaced thermograms; (b) Curve deduced from (a) and used to obtain isothermal cure curve at temperature T_0 .

An isothermal cure curve can be drawn using these curves. An ordinate at T is drawn in each thermogram. The state of the resin is described by three parameters; temperature (T), heat generation rate (dH/dt) and heat of reaction (H). H is given by the shaded area, and the total heat of reaction H_0 is given by the area enclosed by the complete curve. The eight states shown in Figure 2(a) are plotted in reduced forms as shown in Figure 2(b). The integral of the curve from zero to H/H_0 is equal to the time to reach degree of cure H/H_0 at temperature T_0 . Therefore, the isothermal cure curve of H/H_0 versus t can be constructed. This process can be repeated at any temperature but at temperatures lower than T_0 in Figure 2(a) since the final part of the cure curve will be missing. Thus, at low temperature the isothermal method gives reliable results while the scan method gives insufficient data from which to construct a reliable curve. On the other hand, for fast cure or when the curing temperature is too high, the thermograms with different scan rates must be used. The third method is to scan only partly cured resins. Each partly cured sample is scanned and the area of the thermogram gives the residual heat of reaction ($H_0 - H$) from which H could be derived. This method becomes useful when the rate of heat evolution is too small for isothermal detection.

On the other hand, characterization of the kinetics of epoxy resin curing reactions is not only essential for a better understanding of structure-property relationships but also required for determining the time-temperature dependence of the degree of cure. DSC has been used by several workers both to monitor the state of cure and to determine the kinetic parameters of cure of epoxy resins both in isothermal and dynamic modes. There are two interrelated methods for analyzing DSC curves of crosslinking reaction of epoxy resins. The first method utilizes a single DSC thermogram to evaluate the kinetic parameters, such as activation energy (E), kinetic order of reaction (n), and the total heat of reaction (H_0), by detailed differential-integral analysis of the DSC thermogram. The second method uses the multiple DSC scan, obtained at various rates of heating.

The first method was proposed by Ellerstein(61) and is based on the calculation of Borchardt and Daniels(62). The general kinetic equation which is of Arrhenius type is given by the following expression:

$$dx/dt = k(1-x)^n$$

where dx/dt is the rate of reaction, k is the reaction rate constant, x is the extent of cure.

$$\text{Since } k = A \exp(-E/RT)$$

we can rewrite the equation as follows:

$$dx/dt = A \exp(-E/RT)(1-x)^n$$

where A is the frequency factor, E is the Activation energy, R is the gas constant, and T is the absolute temperature. From the assumption that the heat evolved is proportional to the extent of reaction:

$$x = H/H_0 \text{ and}$$

$$dx/dt = d(H)/H_0 dt$$

where H is the partial heat of reaction which varies in direct proportion to the fraction reacted, x , and H_0 is the total heat of reaction which is equal to the total area under the curve.

Combining the above equations gives:

$$dH/dt = A(H_0) \exp(-E/RT)(1-H/H_0)^n$$

In a dynamic DSC run, the heating rate (or scan rate) $G = dT/dt$, so that the above equation can be written as:

$$dH/dt = A(H_0/G) \exp(-E/RT)(1-H/H_0)^n$$

This equation shows the change of degree of cure with temperature. These calculations were extended by Crane and Kaelble(63) to a study of the curing of epoxy resin. They derived the following equation to calculate the kinetic parameters of the system they studied.

$$\left[\frac{d^2H / dT^2}{dH / dT} \right] T^2 = \left[\frac{E}{R} - \frac{nT^2}{(1-x)H_0} \left(\frac{dH}{dT} \right) \right]$$

dH/dt is the ordinate scale of a DSC curve, and it is converted through the scan rate $Q=dT/dt$ to become curve height $h = dH/Qdt = dH/dT$. The term d^2H/dT^2 becomes the slope of the curve, S , at temperature T . Furthermore, from the definition of $x = H/H_0$, the term $(1-x)H_0$ becomes equal $H_0 - H$ which is the remaining area, A , under the DSC curve. By making these substitutions in the above equations, the following equation is obtained.

$$(S/h)T^2 = E/R - nT^2(h/A)$$

After evaluating the values of slope, S , curve height, h , and remaining area A at various temperature, a plot of $(S/h)T^2$ versus $T^2(h/A)$ will be a straight line whose slope defines the order of reaction, n , while the activation energy, E , is obtained from the intercept at $T^2(h/A)=0$

The second method which utilizes multiple DSC curves obtained at various scan rates, is due to Kissinger(64). The method assumes that the reaction rate is a maximum at the peak temperature, T , of a DSC curve. The quantity $h = dH/dT$ attains its maximum value at the peak temperature and the slope $S = d^2H/(dT)^2 = 0$. From the same assumptions stated above, Kissinger obtained the following equation.

$$\frac{d(\ln Q/T^2)}{d(1/T)} = -\frac{E}{R}, \text{ or alternately, } \frac{d \ln Q}{d(1/T)} = -\frac{E}{R} - 2T$$

where Q is the scan rate and T is the peak temperature of the DSC curve. A plot of $\ln Q$ versus $1/T$ from several DSC curves should be linear and the activation energy, E , is obtained from the slope when $E/R \gg 2T$. It should be noted that the activation energy is determined by using the above equation regardless of order of reaction which is assumed to remain constant throughout the reaction.

It is obvious that the kinetic order(n), activation energy(E), and heat of reaction of a curing system can all be defined using a single DSC curve at a constant scan rate by using the above equations. The great advantages of the Kissinger method is to evaluate the effects of scan rate on the cure kinetics. Therefore, a combined analysis using these two interrelated methods provides a more comprehensive evaluation of the curing kinetics in epoxy resin systems.

Most research on the cure kinetics of epoxy resin system was without fillers(18-25). Very little information has been reported on epoxy systems containing fibers by DSC. Pappalardo(26) used DSC to determine the activation energy and reaction rate constants for some epoxy-glass fiber composites. The effect of filler on the curing behavior was found to depend on the specific filler and polymer system. Dutta and Ryan(27) used DSC to investigate the effect of carbon black and a silica filler on the cure kinetics of a model epoxy resin cured stoichiometrically with an aromatic diamine. They found that the filler does not significantly affect the order of the reaction but does influence the reaction rate. It appears that the carbon black fillers affect kinetic rate constants through the Arrhenius frequency factor, whereas the surface-treated silicas influence the kinetic rate constants through the activation energy. C. H. Smith(28) used DSC to evaluate cure and shelf life of epoxy preregs, and correlate the total heat of reaction to resin flow to predict the processing characteristics.

The most serious problem(29) with DSC is the requirement of an accurate knowledge of the base line. The base lines are always taken at locations preceding and following the exotherm. However, the base lines should take into account the change in heat capacity of the cured resin compared to starting materials. Schneider and Gillham(29) have studied the curing behaviors of two dicy-containing epoxy resins. As shown in Figure 3, the DSC scan of epoxy resins that consist of DGEBA(diglycidyl-ether of bisphenol A), novalac, and amine as curing agent. The baseline which represents the scan of the cured resin, is lower than the uncured resin at the starting point, then undergoes an upward endothermal shift at the glass transition temperature(107°C) and stay above the initial scan for the higher temperature. Therefore, it is impossible to produce an accurate extrapolation from the cure curve to get the correct baseline. If the base line is taken as the tangent to the DSC curve at a location preceding and following the exotherm, then the heat of reaction is 71 cal/g. On the other hand, if the extrapolation is done as shown, by the portion of the curve between the arrows, the value obtained is 91 cal/g, which is very close to the result obtained by isothermal curing runs at higher temperature. It is obvious that the results are quite different with different baselines. Since it is impossible to get a correct baseline, only an approximation of the heat of reaction can be

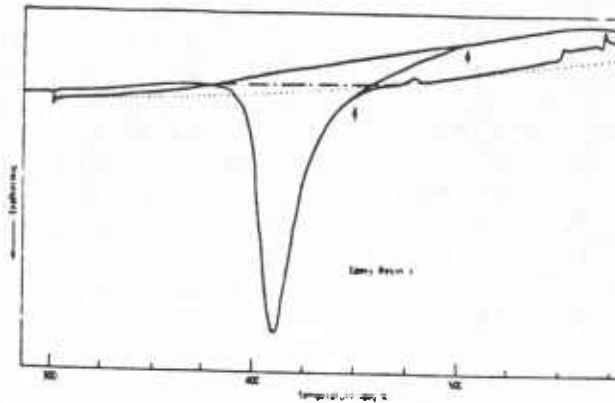


Figure 3. DSC scan of resin 1 showing cure curve and various baselines. Full curves, scan of cured and uncured resin; dotted curve, scan with empty sample cells; chain curve, tangent to cure peak. Arrows indicate extrapolation of cure curve to baseline represented by scan of cured resin.

obtained from the scanning runs. In other cases where the scan shows complex behavior, such as that shown in Figure 4. The resin used for Figure 4 is a mixture of DGEBA, novalac, TQMDA (tetraglycidyl methylenedianiline). It shows a major exotherm appears at 141° C, a broad and smaller exotherm peaking at 236° C, and a third peak starting at 260° C. The exotherm above 260° C arises from sample degradation. It is obvious that any determination based on the tangent base lines rather than from the baseline produced by rescan of the cured epoxy resin will be in error. The problem of estimating the conversion is even more complicated in this case. It involves the resolution of the two lower temperature exotherms. J.F. Sprouse estimated the extent of reaction occurring in the second curing region. The value obtained is too high compared with FTIR result (38 vs 24 percent). Since the infrared measurement is considered more reliable than the value extracted from DSC. Sprouse(29) used 24 percent conversion from FTIR results and calculated the total heat of reaction from the lower limit, and got 20 kcal/mole. Compared with the results from the literature, which has a value of 26 kcal/mole, it implies that the area from the DSC curve for calculating the percent conversion could lead to the result that is 30 percent too low. On the other hand, the deviation of the DSC results is about 1%.

Compared with DSC, DTA(30) is seldom used in the study of epoxy resins. It was shown that there is a good correlation between the gelation time and the temperature corresponding to the peak of the exotherm on DTA curves. The DTA method permitted a rapid and sufficiently accurate estimate of gelation time of epoxy resin in a broad temperature range.

Isothermal DSC provides the heat output as a function of time, representing directly the rate of the reaction. However, the information provided by this method gives us little insight into the chemical mechanism of the curing process and the chemistry of cure.

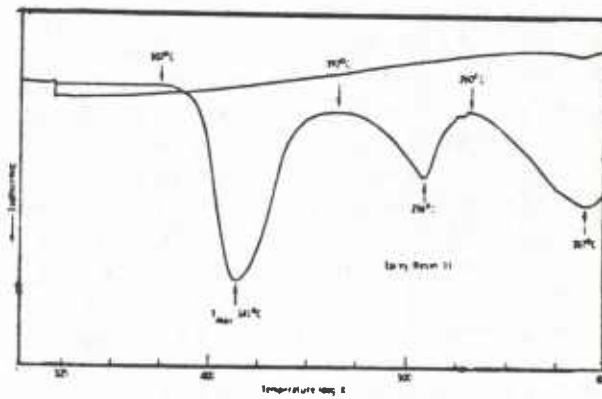


Figure 4. DSC scans of resin II (see text). Heating rate 5°C/min. 320 to 600°K, atten. 10 mcal/s, sample wt 13.1 mg.

4.0 DYNAMICAL MECHANICAL TESTS

One of the most important factors affecting the processing of the epoxy resins is gelation. When gelation begins, the viscosity of the system rises exponentially and has a remarkable effect on the processing such as injection molding or auto-claving. A typical method for determining time to gelation is by a standard ASTM(31) test, which is based on steady-state viscosity. A schematic representation for the cure behavior of an epoxy system is shown in Figure 5. Steady-state viscosity measurements only characterize the liquid state. Characterization of the rubbery and glassy states can be made with dynamic mechanical techniques.

Torsional Braid Analysis(TBA), a dynamical mechanical technique(30), involving an adaptation of the torsional pendulum with a freehanging composite specimen consists of a multifilamented glass braid and the epoxy system. With this technique, we can measure the change in rigidity and damping in the reacting system throughout the cure, and study transitions during cure, cure kinetics, and activation energy.

Two physical transitions are usually observable with TBA as cure proceeds isothermally. The first, gelation, corresponds to a transition from linear or branched molecules to an infinite network. The second, vitrification, corresponds to a transition from a rubbery to a glassy state. Each of these phenomena is accompanied by an increase in rigidity and by a maximum in mechanical damping. There exist two critical isothermal temperatures. These are $T(g_{\infty})$ (the maximum glass transition temperature) and $T(gg)$ (the glass transition temperature at its gel point). As shown by J.K. Gillham: only gelation is observed, if $T(\text{cure}) > T(g_{\infty})$; both gelation and vitrification are observed, if $T(g_{\infty}) > T(\text{cure}) > T(gg)$; only vitrification is observed, if $T(\text{cure}) < T(gg)$. This information is related to the rheological changes which occur during the complete cure of the epoxy resin and are useful in composite processing. As shown in Figure 6, a typical TBA interpretation.

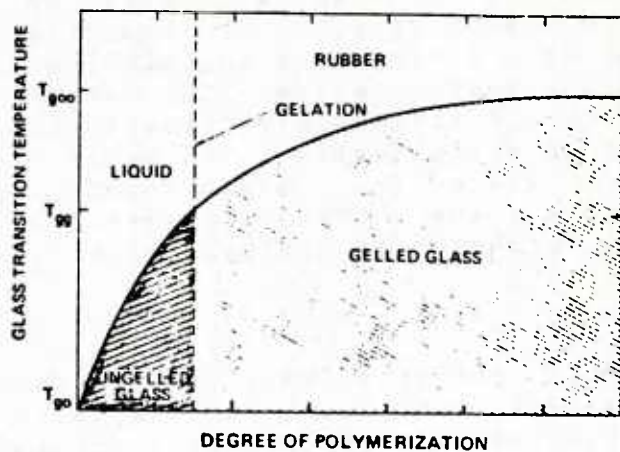


Figure 5. Glass transition temperature vs. degree of polymerization for a thermosetting system.

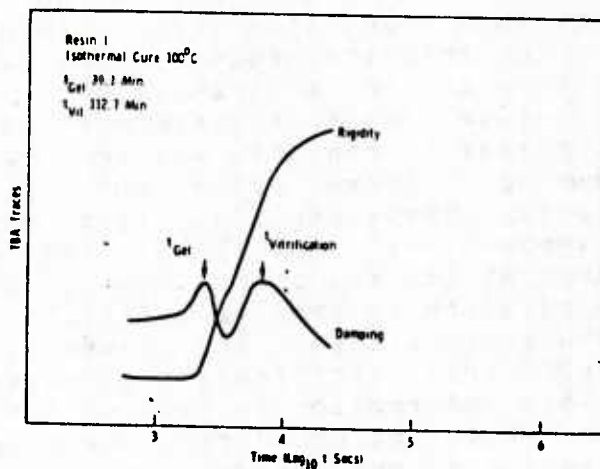


Figure 6. Relative rigidity and damping curves vs time for the reaction of resin 1 at 100°C.

A number of studies(32-34,29) have been reported on the curing behavior of epoxy resins employing TBA. Quite a few of the studies are concerned with mixture of fiber and epoxy. J.K.Gillham(35) used TBA to study the prepreg material consisting of epoxy resin on glass fiber, carbon fiber, or aramid fiber, and measured gelation and vitrification times as a function of temperature. The study has shown that substantially all of the information concerning the curing behavior of epoxy resins, which has been obtained by TBA, can also be obtained on the prepreg material directly. The only difference is a marked weakening of the gelation mechanical damping peak in the prepreg material. In spite of its weak intensity, the gel points still can be constructed very accurately to determine the activation energy by plotting an Arrhenius equation over a wide range of temperature. It is obvious that the filler does not affect the behavior significantly nor does it interfere with the results under study.

In addition to torsional braid analysis, there are other similar techniques. W.J.Macknight(36) used dynamic spring analysis to study the curing behavior of two commercially formulated epoxy resins. It is demonstrated that this supported viscoelastic technique is suitable for the determination of the onset of gelation but the method is not useful for studying later stages of reaction when the resins become more rigid. I.J.Goldfarb(37) studied the curing behavior with torsion impregnated cloth analysis. This method used glass cloth as a resin support, monitoring the dynamic mechanical properties of resins during the curing process. In spite of the similarity between TBA and this technique there are some differences between these two techniques. Torsional Impregnated Cloth Analysis (TICA) has some advantages over TBA. Its frequency of measurement is constant, and the frequency can also be varied to study the frequency effect on transition. In TBA, the resin impregnated braid is set in free oscillatory motion and its damping decay characteristic is recorded. The frequency of oscillation can be related to the storage modulus(G') of the resin while the log of the amplitude decrement is proportional to the $\tan \theta$ (where θ is phase angle between stress and strain). On the other hand, in the TICA experiment the cloth undergoes an oscillatory strain at a fixed frequency, and the resultant torque is analyzed by a frequency response analyser to give

both the in-phase and out-of-phase component amplitudes. The results obtained from TICA are not absolute values, and have the advantage over the TBA in that the frequency of measurement is constant. The frequency can be varied to study the frequency effect on the transitions. Another advantage is that in TBA the rigidity may be influenced by substrate-resin interactions(38), while in TICA the in-phase and out-of-phase components are measured directly, so the loss modulus transition can be identified more confidently.

Tung and Dynes(39) used a visco-elastic tester to perform the dynamical test. Since a disadvantage of this kind of dynamical mechanical approach is that gelation is not clearly observed, they described a method for determining the gel time of epoxy resins from dynamic viscoelastic data, which is based on the crossover of the dynamic storage G' and loss G'' moduli measured during isothermal curing. As shown in Figure 7, the dynamic mechanical properties of the 171°C isothermal cure of a dicycrosslinked epoxy resin. The two modulus curves intersect, i.e., ($G''=G'$ or $\tan \theta = 1$) at $t=1.8$ min. It was found, however, that the time to reach the modulus crossover point ($\tan \theta = 1$) coincides with the gel time as measured by the standard gel time test. Further examples of this correlation are shown in Figure 8 for a variety of crosslinking systems varying widely in gel time. This correlation suggests a loss tangent ($\tan \theta$) of unity at the gel point. Loss tangent, being the ratio of energy lost to energy stored in a cyclic deformation ($\tan \theta = G''/G'$), measures the relative contribution of elasticity and viscosity of an epoxy system. $\tan \theta$ of a viscous liquid should therefore be greater than 1, while that of an elastic solid should be less than 1. When the cure temperature is above $T(gg)$, resin system proceed from a viscous liquid through gelation to elastic solid. Under these conditions, $\tan \theta$ of gelation, the transition state between viscous liquid and elastic solid, would be expected to be equal to 1. As demonstrated by Tung and Dynes, this method is more precise and free of operation error than the conventional method in the determination of gel times of epoxy resin.

Another application of dynamic mechanical test is the characterization of cured composites. The useful information can be obtained is the glass transition temperature. As demonstrated by Katherine E. Reed(40), the most interesting observation was the appearance of an additional damping peak above the glass transition temperature of the matrix resin.

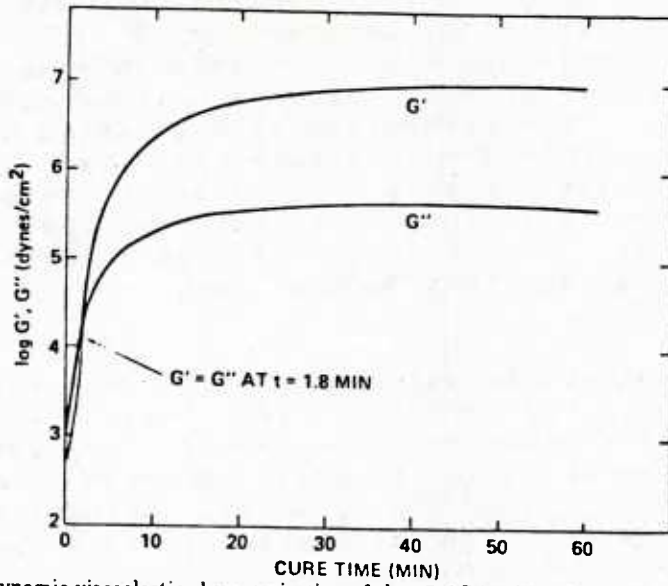


Figure 7. Dynamic viscoelastic characterization of the 171°C isothermal curing of a DICY cured epoxy resin at 10 rad/s and 10% strain.

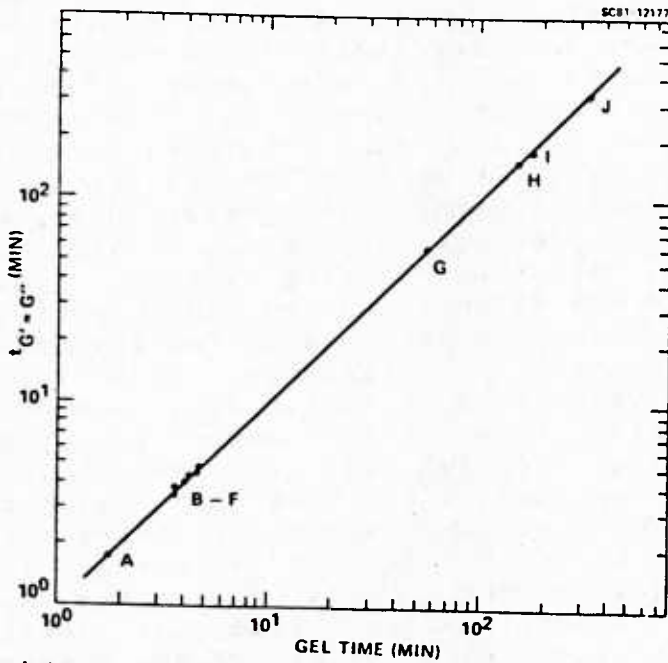


Figure 8. Correlation of gel time and time of modulus crossover of thermosetting resins. (A) brominated epoxy, $T_{cure} = 171^{\circ}C$; (B)-(F) epoxy, $T_{cure} = 171^{\circ}C$; (G) AT'S, $T_{cure} = 150^{\circ}C$; (H)-(I) silicones, $T_{cure} = 25^{\circ}C$.

Also, as the fiber direction was changed from transverse(90°) to longitudinal(0°), the transition region broadened and the change in frequency over this temperature range exhibited a maximum at intermediate angles. This phenomenon is associated with the unique resin layer in the interface which has been estimated to comprise roughly 0.1 % of the total resin in the composite, assuming thickness on the order of 100 Angstroms. The structure of this interfacial region is different from that farther away.

Dynamic mechanical tests can be used to detect gelation and vitrification that are the the key parameters which describe the curing behavior. They are useful in prepreg technology and composite processing. However, dynamical mechanical tests can not provide the necessary information about the curing chemistry and curing mechanism

5.0 SPECTROSCOPY

5.1 Introduction:

Introduction: Infrared spectroscopy has long been recognized as a powerful tool for monitoring the curing process and to characterize the cured epoxy composites. It is based on the absorption of radiation in the infrared frequency range due to the molecular vibrations of the functional groups contained in the polymer chain. Prior to FT-IR, infrared spectroscopy was carried out using a dispersive instrument utilizing prisms or gratings to geometrically disperse the infrared radiation. Using a scanning mechanism, the dispersed radiation is passed over a slit system which isolate the frequency range falling on the detector. In this manner, the spectrum, that is, the energy transmitted through a sample as a function of frequency is obtained. This infrared method is highly limited in sensitivity because most of the available energy is being thrown away, i.e., does not fall on the open slits. For polymer analysis, where the bands are generally broad and weak, this energy limitation is particularly severe. Hence, to improve the sensitivity of infrared spectroscopy, FTIR was developed, which allows the examination of all of the transmitted energy all of the time.

5.2

Fourier Transform Infrared Spectroscopy--description of method

Fourier Transform Spectroscopy uses the Michelson interferometer rather than the conventional grating instruments. The Michelson interferometer has two mutually perpendicular arms. One arm of the interferometer contains a stationary, plane mirror; the other arm contains a movable mirror. Bisecting the two arms is a beamsplitter which splits the source beam into two equal beams. These two light beams travel down their respective arms of the interferometer and are reflected back to the beam splitter and on to the detector. The two reunited beams will interfere constructively or destructively, depending on the relationship between their path difference (x) and the wavelengths of light. When the movable mirror and the stationary mirror are positioned the same distance from the beam splitter in their respective arms of the interferometer, the paths of the light beams are identical. Under these conditions all wavelengths of the radiation striking the beam splitter after reflection add coherently to produce a maximum flux at the detector and generate what is known as the center burst. As the movable mirror is displaced from this point, the path length in that arm of the interferometer is changed. This difference in path length causes each wavelength of source radiation to destructively interfere with itself at the beam splitter. The resulting flux at the detector, which is the sum of the fluxes for each of the individual wavelengths, rapidly decreases with mirror displacement. By sampling the flux at the detector, one obtains an interferogram. For a monochromatic source of frequency ν , the interferogram is given by the expression :

$$I(x) = 2R(\nu)T(\nu)I(\nu)(1 + \cos 2\pi\nu x)$$

where $R(\nu)$ is the reflectance of the beam splitter, $T(\nu)$ is the transmittance of the beam splitter, $I(\nu)$ is the input energy at frequency ν and x is the path difference. The interferogram consists of two parts, a constant (DC) component equal to $2R(\nu)T(\nu)I(\nu)$ and modulated (AC) component. The AC component is called the interferogram and is given by

$$I(x) = 2R(\nu)T(\nu)I(\nu)\cos 2\pi\nu x.$$

An infrared detector and AC-amplifier converts this flux into an electrical signal

$$v(x) = \text{Re } I(x) \text{ volts}$$

where Re is the response of the detector and amplifier.

For highest accuracy in the digitized signal, the maximum intensity in an interferogram should match as closely as possible the maximum input voltage of the analog/digital converter (ADC). The noise must also be given at least four or five units, so the computer word length in FT-IR spectrometers is 16 (or 32 in double precision), 20 and 24 bits. Griffiths(41) gives the example of measuring the spectrum of a continuous source whose intensity is uniform from 4000 to 400 cm^{-1} and zero outside this band. The signal-to-noise ratio of the spectrum $(S/N)_S$ is related to the signal-to-noise ratio of the interferogram $(S/N)_I$ by

$$(S/N)_I = M^2 (S/N)_S$$

where M is the number of resolution elements. So if we want to measure the spectrum with a $(S/N)_S = 500$ at resolution 1 cm^{-1} ($M=3600$) in a single scan, S it can readily be seen that $(S/N)_I = 3 \times 10^4$ and the full dynamic range of a 15-bit ADC (2^{15}) is only large enough to adequately digitize the signal. If $(S/N)_I$ were any greater than 30000 the noise level in the digitized interferogram is set by the least significant bit of the ADC rather than by detector noise. For this reason, minicomputer with a wordlength as large as 20 bits are required so that a reasonable number of scans can be signal averaged.

The interferogram for a polychromatic source $A(v)$ is given by

$$I(x) = \int_{-\infty}^{+\infty} A(v) \left\{ 1 + \cos 2(\pi vx) \right\} dv$$

The methods of evaluating these integrals involve a determination of the values at zero-path length and very long or infinite path length. At zero difference

$$I(x) = 2 \int_{-\infty}^{+\infty} A(v) dv$$

and for large path differences

$$I(x) = \int_{-\infty}^{+\infty} A(v) = I(0)/2$$

so the actual interferogram $F(x)$ is

$$F(x) = I(x) - I(\infty) = \int A(v) \cos 2(\pi vx) dv$$

From Fourier transform theory

$$A(v) = 2 \int_{-\infty}^{+\infty} F(x) \cos(2\pi vx) dx$$

This Fourier transform process was well known to Michelson and his peers but the computational difficulty of making the transformation limited the application of this powerful interferometric technique to spectroscopy. An important advance was made with the discovery of the fast Fourier transform algorithm by Cooley and Tukey(42). The use of the FFT revived the field of spectroscopy using interferometers by allowing the calculation of the Fourier transform to be carried out rapidly. The essence of the technique is the reduction in the number of computer multiplications and additions for n data points. The normal computer evaluation requires $n(n-1)$ additions and multiplications whereas the FFT method requires $(n \log_2 n)$ additions and multiplications. If we have a 4096-point array to Fourier transform, it would require $(4096)^2$ or 16.7 million multiplications. The FFT allows us to reduce this to $(4096) \times \log_2 (4096)$ or 49152 multiplications, a saving of a factor of 341 in time. The advantage of the FFT increase with the number of data points. As computers have improved the time required for a Fourier transform has reduced until currently the transformation can be carried out in less than a second with fast array processors, thus the spectra can be calculated during the return of the moving mirror if desired.

However, it is to be noted that the Fourier transform integrals have infinite limits while the optical path difference are finite so modifications or approximations must be made. We will use the approximation of the limits between $-L$ and L where L is the maximum distance of the mirror drive. So

$$S(v) = 2 \int_{-L}^{+L} F(x) \cos 2\pi vx dx$$

where $S(v)$ is used to indicate that we are approximating the Fourier transform. It is of interest to examine the effect of this finite optical path length approximation on the $S(v_K)$ of an incident monochromatic source of wavelength v_K . The interferogram for this source is

$$F(x) = A(v_K) \cos 2\pi v_K x$$

where $A(v_K)$ is the amplitude of the light intensity. Making the substitution, we obtain

$$S(v_K) = 2 \int A(v_K) \cos(2\pi v_K x) \cos(2\pi v x) dx$$

and after the transformation one obtains

$$S(v_K) = A(v_K) 2L \operatorname{sinc} 2\pi(v_K - v)L$$

where the sinc function of y is $\sin y/y$. This function represents the instrument line shape of a Michelson interferogram. Obviously, this instrument line shape is not satisfactory because of the strong side lobes. These side lobes can be removed by apodization. Apodization is carried out by multiplying the interferogram by a function $H(x)$, before the Fourier interferogram is transformed. Thus;

$$S(v) = 2 \int_{-L}^{+L} F(x) H(x) \cos(2\pi v x) dx.$$

A variety of apodization functions(43,44) have been examined. Triangular apodization has the following form:

$$H(x) = 1 - |x|/L \text{ if } x \leq L \text{ and zero otherwise.}$$

Again for a monochromatic source, we have

$$S(v) = 2 \int_{-\infty}^{+\infty} A(v_K) \left(1 - \frac{|x|}{L}\right) \cos(2\pi v_K x) \cos(2\pi v x) dx$$

Note that the integration limits could now be changed to plus and minus infinity without changing the result, because the integrand is zero outside of the range $-L \leq x \leq L$, integration yields

$$S(v) = A(v_K) L \sin^2(v_K - v)L$$

A summary of the effects of apodization has been given and recommendations(45) made for the appropriate apodization function for quantitative infrared measurements. There are a number of other problems such as phase correction arising from the fact that in

practice, the radiation undergoes phase shifts due to beamsplitter characteristics, signal processing delays, refraction effects in materials and so forth. Several techniques have been developed which allow appropriate corrections to be made for these effects(46).

The advantages of FT-IR over grating infrared arises from several sources. For measurements taken at equal resolution and for equal measurement time with the same detector and optical throughput, the signal-to-noise(S/N) of spectra from an FT-IR will be M times greater than on a grating instrument where M is the number of resolution elements being examined during the measurement. Alternately, for a given observation time, it is possible to repeat the FT-IR measurement M times which increases the signal by a factor of M and the noise by a factor of $M^{1/2}$, to achieve a S/N enhancement of a factor of $M^{1/2}$. This advantage arises from the fact that the FT-IR spectrometer examines the entire spectrum in the same period of time required for a dispersive instrument to examine a single spectral element. Theoretically, an FT-IR can acquire the spectrum with the same S/N from 0 to 4000 cm^{-1} with 1-cm resolution 4000 times faster than a dispersive instrument. Or from another point of view, for the same measurement time a factor of approximately 63 increase in S/N can be achieved on the FT-IR instrument. Therefore, when there is a limited time for measurement, there is a definite time advantage for the FT-IR. When time of measurement is not an important consideration, the time can be used to multiscan with an FT-IR to signal average and increase the S/N. Of course, there is also the inherent time advantage associated with rapid scanning FT-IR since it requires a very short time to obtain the complete spectra(1.5 sec). This time advantage of the FT-IR has been particularly important for the study of the curing reaction of epoxy resins and degradation process and other time-dependent processes of epoxy resin.

Another advantage of FT-IR comes from the fact that the frequencies of an FT-IR instrument are internally calibrated by a laser whereas conventional IR instrument exhibit drifts when changes in alignment occur. This advantage is particularly useful for coaddition of spectra to signal average since the frequency accuracy is a requirement in this case. For the absorbance subtraction technique to be useful for epoxy resins examined over a period of time such as

months or years, long term frequency accuracy must be maintained. Applications such as quality control and long term aging and weathering require the reproducibility of the frequency that can be achieved by FTIR instrument over the long term.

The overall simplicity of an FT-IR compared to a dispersive instrument is also an advantage. For example, a single instrument can be easily converted to study the near, mid or far-infrared frequency regions whereas with the dispersive method, three totally different instrument are required. To improve resolution with an FT-IR instrument, the basic design is only slightly modified while for a dispersive instrument different optical components are required. This is important, since in cases where interfering absorptions are present in the epoxy resins, the near-IR may be very useful to characterize epoxy content at 4535 cm and hydroxyl content at 6784 cm.

5.3 Quantitative Infrared Measurements:

Quantitative IR methods are based on the Beer-Lambert Law,

$A = E \times C$, where A is the absorbance for unit pathlength, E is the extinction coefficient, C is the concentration. The analysis of any multicomponent resin or composite is greatly facilitated if the spectrum of that material may be expressed by a linear combination of a finite set of pure component spectra. The entire process may be separated into three steps: calculation of the number of species present, identification of each of those species, and a suitable fitting of the spectra of those species to the spectra of composites. The factor analysis methods are useful in determining the number of spectroscopically distinguishable components in the composites.

5.4 Factor Analysis of Mixture:

Factor analysis is based upon expressing a property as a linear sum of terms called factors and the technique has found wide application to a variety of multidimensional problems. The technique has been applied to infrared and Raman spectra and most recently to FT-IR spectra.

The Beer-Lambert law can be written for a number of components over a wave length range as:

$$A_i = \sum_j^n \epsilon_j c_{ij}$$

where A_i is the absorbance spectrum of mixture i , ϵ_j is the absorptivity for the j th component, and c_{ij} is the concentration of component j in mixture i . Factor analysis is concerned with a matrix of data points. So in matrix notation we can write the absorbance spectra of a number of solutions as:

$A=EC$ where A is a normalized absorbance matrix which is rectangular(rxp) in form having columns containing the r absorbance at each wavenumber r recorded and the p rows corresponding to p different mixture being studied. The A matrix could thus be 400 by 10 corresponding to a measurement range of 400 wavenumbers at one wavenumber resolution for 10 different mixtures or solutions. E is the molar absorption coefficient matrix(rxn) and conforms with the A matrix for the wavelength region, but only has n rows corresponding to the number of absorbing components. C is the concentration matrix (nxp) and has dimensions of the number of components, n , by the number of mixtures or solutions, p , being studied. Of course, we do not know E and C or we would not have a spectroscopic problem since E and C contain all of the information required to interpret A . Factor analysis can be used to generate E and C which allows a complete analysis of a series of mixtures containing the same components in differing amounts.

There are two basic assumptions in factor analysis. First, the individual spectra of the components are not linear combinations of those of the other components and secondly, that the concentration of one or more species cannot be expressed as a constant ratio of another species. It is the different relative concentrations of the components in the mixtures that provides the additional information necessary to deconvolute the spectra.

What factor analysis allows initially is a determination of the number of components n in the p mixtures required to reproduce the absorbance or data matrix A . In factor analysis we find the rank of the matrix A and the rank of A can be interpreted as being equal to the number of absorbing components. To find

the rank of A, the matrix $M = A^T A$ is formed where A^T is the transpose of A. This matrix termed the covariance or second moment matrix has the same rank as A, but has the advantage of being a square matrix ($p \times p$) with the dimensions corresponding to the number of solutions or mixtures being examined. In the absence of noise, the rank of A is given by the number of nonzero eigenvalues of M.

5.5 Least Squares Quantitative Analysis of Infrared Spectra:

Since the set of pure components spectra determined are linearly independent, they may be unambiguously fitted by a least-squares criterion to the spectrum of the composite. The least-squares algorithm is derived from the criterion of minimization of the sum of squared differences between the experimental and the fitted spectra. The algorithm employed is a simple linear regression model for gamma-spectra:

$$\sum_{i=1}^N R_{i,k} = \sum_{j=1}^M X_j \left(\sum_{i=1}^N W_i R_{i,j} R_{i,k} \right)$$

In this equation N=number of data points in each spectrum, M=number of standard spectra, $R_{i,k}$ =datum in the i^{th} channel of the k^{th} standard spectrum, S_i datum in the i^{th} channel of the composite spectrum, $W_i = 1/S_i$, =weighting factor, and X_j =number to be determined such that the sum of all standard (pure component) spectra, when multiplied by their X_j values, gives a best least-squares fit to the composite spectrum. The least-squares coefficients as derived are useful in determining proper scaling factors for absorbance subtraction techniques in FTIR. If the pure component spectra are properly scaled, then the least-squares coefficients yield the correct volume fractions (or weight or mole fractions, if desired) for a composite consisting of any mixture of those components. Besides, if the quality of the least-squares fit within random error, then a statistical error analysis may be performed to determine confidence intervals for each least-squares coefficient.

5.6 Absorbance Subtraction Method:

One of the spectral processing operations most widely used in polymer analysis is the digital subtraction of absorbance spectra. In order to reveal or emphasize subtle difference between two samples or a

sample and a reference material. Spectral subtraction with FTIR is a powerful method of extracting structural information about components of composite spectra. When the epoxy resin is examined before and after a chemical or physical treatment, and subtracting the original spectrum from the final spectrum, positive absorbances reflect the structures that are formed during the treatment and negative absorbances reflect the loss of structure. The advantage of FT-IR difference spectra lies in the ability to compensate for difference in thicknesses of the two solid samples. This balance of thicknesses allows small spectral difference to be associated with structural changes and not be outweighed by the difference in the amount of sample in the beams. Additionally, with properly compensated thickness, the differences in absorbances can be magnified through computer scale expansion to reveal small details of the spectral differences. The scaling parameter, k , is chosen such that:

$$(A_1 - kA_2) = 0$$

where A_1 and A_2 correspond to the absorbances of the internal thickness bands of samples one and two. Multiplication of the absorbance spectrum of sample 2 by k will yield a new spectrum having the same optical thickness as sample one. One may use the peak absorbance, integrated peak areas, or a least-squares curve fitting method to calculate the scaling factor k .

E. M. Pearce (47) demonstrated the subtraction method of FTIR to compare the functional group stability of epoxy resins. This is based on the following considerations:

If two functional groups x and y decrease their IR spectral absorbance at the characteristic frequency ν and ν' , the difference absorbance of each functional group can be expressed as

$$A_s^{\nu_x} = A_2^{\nu_x} - k A_1^{\nu_x}$$

$$A_s^{\nu_y} = A_2^{\nu_y} - k A_1^{\nu_y}$$

In order to remove functional group x from the difference spectrum, the k' parameter can be obtained:

$$k' = A_2^{\nu_x} / A_1^{\nu_x} = C_2 / C_1$$

where C is the concentration of the functional group x. Three situations can occur in relation to the absorbance of the functional y:

$$A_s^{\nu_y} - k' A_1^{\nu_y} = e_y b (C_2 - k' C_1) \gtrless 0$$

where e_y is the extinction coefficient.

If the value is more than zero, the group y is more stable than the group x; if as stable as ($=0$) or less stable than group x (< 0), respectively, under specific degradations.

5.7 Sampling Techniques for FT-IR:

Transmission spectroscopy, Diffuse Reflectance spectroscopy, and Internal-Reflection spectroscopy can be used to characterize the epoxy resin in composites.

The optics of the sampling chamber of commercial FT-IR instruments are the same as the traditional dispersive instruments so the accessories which are generally available commercially can be used. The main difference between the two types of instrumental optics is that the beam is round and larger at the focus for FT-IR. Thus, some of the sampling accessories may block some of the beam energy in FT-IR experiments. When energy is a limiting factor, the accessories can be modified to accommodate the larger beam. However, the improved sensitivity of FT-IR allows one to obtain better sensitivity using the conventional sampling accessories and expand the range of sampling techniques.

In internal reflection spectroscopy (IRS) the sample is in optical contact with another material (e.g. a prism). The prism is optically denser than the sample, the incoming light forms a standing wave pattern at the interface within the dense prism medium, whereas in the rare medium the amplitude of the electric field falls off exponentially with the

distance from the phase boundary. If the rare medium exhibits absorption, the penetrating wave becomes attenuated, so the reflectance can be written:

$$R=1-kd_c$$

where d_c is the effective layer thickness. The resulting energy loss in the reflected wave is referred to as attenuated total reflection (ATR). When multiple reflections are used to increase the sensitivity, the technique is often called multiple internal reflection (MIR). Thus qualitatively, an IRS spectrum resembles a transmission spectrum. There are two adverse effects arising from the wavelength dependence of IRS. First, the long wavelength side of an absorption band tends to be distorted and second, bands of longer wavelengths appear relatively stronger. With FT-IR spectrometers, one does not achieve the same improvement in IRS as in transmission compared to dispersion instruments because the ATR attachments have not been redesigned for the larger, round beam. However, the signal averaging capability and speed have increased the utility of IRS for polymers particularly for surface studies. In IRS, the infrared beam penetrates the surface of the composite between a few tenths of a micron to a few microns depending on the type of reflection plate, the angle of incidence, and the wavelength of the infrared beam. The depth of beam penetration can be reduced by placing a thin barrier film between the trapezoidal reflection plate and the epoxy resin under study. Hirschfeld has generated the algorithms which are necessary to use IRS to determine the optical constants of a sample from a pair of independent reflectivity measurements at each frequency. The optimum method appears to be to determine the total reflectance at two polarizations at the same incidence angle. Another important sampling technique is Diffuse Reflectance Measurements. When light is directed onto a sample it may either be transmitted or reflected. Hence, one can obtain the spectra by either transmission or reflection. Since some of the light is absorbed and the remainder is reflected, study of the diffuse reflected light can be used to measure the amount absorbed. However, the low efficiency of this diffuse reflectance process makes it extremely difficult to measure and it was initially speculated that infrared diffuse reflectance measurements would be futile. Initially, an integrating sphere was used to capture all of the

reflected light but more recently improved diffuse reflectance cells have been designed which allow the measurement of diffuse reflectance spectra using FT-IR instrumentation.

The requirement for reflectance to be diffuse is that the intensity of reflected light is isotropic but for a solid sample both scattering and absorption occur, and since the scattered radiation is angularly distributed, it is by no means isotropic. However, with a large number of particles, as is found in a powder, an isotropic scattering distribution can be achieved, so the emerging light will still be diffuse. Kubelka and Munk used an empirical theory to relate the absorption coefficient (k) and the scattering coefficient (s).

$$f(r_{\infty}) = (1 - r_{\infty}) \frac{k}{s}$$

where r_{∞} is the absolute reflectance of an infinitely thick layer. In practice a standard is used and the following ratio is calculated:

$$r'_{\infty} = r'_{\infty}(\text{sample}) / r'_{\infty}(\text{standard})$$

The principle problem with diffuse reflectance is that the specular component of the reflected radiation, that which does not penetrate the sample, is measured along with the diffuse reflected light which penetrates the sample. Generally, the change in specular reflection with frequency is small except in regions of strong absorption bands where the anomalous dispersion leads to restrahlen bands in the specular reflection spectrum. When the restrahlen bands are observed, the absorption bands can appear inverted at their center. This effect makes quantitative measurements on samples with strong absorptivity very difficult.

For powdered samples, diffuse reflectance offers considerable advantage particularly since no sample preparation is required which could change the morphology of the sample.

6.0 BAND ASSIGNMENTS FOR EPOXY RESINS

Some general assignments for common epoxy system can be found in Handbook of Epoxy Resins by Lee and Neville. The literature contains several reports assigning characteristic absorptions to the epoxide

group in small molecules. As shown in Table 1, the infrared and Raman assignments for Epon 828 and NMA (Nadic Methyl Anhydride) by Antoon and Koenig(48). Absorption decreases due to the reacting species during the crosslinking reaction may be observed at 3008 cm^{-1} assigned to $\nu_s(\text{CH}_2)$ of the epoxide ring], at 1858 and 1780 cm^{-1} [$\nu_s(\text{C}=\text{O})$ and $\nu_{as}(\text{C}=\text{O})$ of the anhydride ring], and 916 cm^{-1} (epoxide ring). Intensity increases after the crosslinking reaction are at 2963 cm^{-1} [$\nu_{as}(\text{CH}_2)$ adjacent to the ester group], at 1743 [$\nu(\text{C}=\text{O})$ ester], and at 1778 cm^{-1} [$\nu(\text{C}-\text{O})$ of the ester]. Table 2 shows the IR spectra of three epoxy resins after curing and before degradation by Pearce(47). The 3550 cm^{-1} band for the resins was assigned to stretching the -OH group. The absorptions at 3060 cm^{-1} and 3036 are due to C-H stretching of the $-\text{CH}_3$ group. C-H stretching of the $-\text{CH}_2-$ group can be assigned to 2933 and 2878 cm^{-1} . The absorption at 1732 may be assigned to stretching the carbonyl groups in DGEBA and DGEBAF. Bands at about 1610 and 1578 cm^{-1} are derived from quadrant stretching of the benzene rings.

7.0 INFRARED STUDIES OF CURING OF EPOXY RESINS

The studies of curing of epoxy resins with infrared spectroscopy are based on the absorption intensity of the epoxy, anhydride and hydroxyl functional groups that appear at 913, 1858, 345 cm^{-1} , respectively. In other cases the near-IR spectra of the epoxy functional group is used. Since the glass fiber has a strong absorption in the mid-IR region, it is very difficult to measure the IR spectra of epoxy matrices with dispersive spectrometers for glass fiber-reinforced composites. Perkinson(49) developed a method of separating the epoxy resin from the cured fiberglass-epoxy composites. The method is based on the concept of differential floatation which involves the separation of two materials of different specific gravity with a liquid of intermediate specific gravity. Infrared spectra of three differently prepared specimens of the same lot of prepreg composite were compared and the results demonstrate the feasibility of this approach for cured composites. The low signal-to-noise resolution limit and the time of scanning the entire spectrum with a dispersive instrument, limits the application of conventional IR to the study of reaction with short half lives. Since FTIR can solve this kind of problem with rapid scanning(1sec), Buckley and Roylance(7) demonstrated this technique by studying the kinetics of a sterically hindered amine-cured epoxy resin systems. Variation in

TABLE 1(a)

INFRARED AND RAMAN BAND ASSIGNMENTS FOR EPON 828

IR	RAMAN	ASSIGNMENT	IR	RAMAN	ASSIGNMENT
~3500		$\nu(\text{OH})$	1457	1462	$\nu(\text{C}=\text{C}) \phi +$
	3210w				$\delta_{\text{as}}(\text{CH}_3)$
	3151w		1431w	1429	$\delta(\text{OCH}_2)?$
3123vw	3125w		1414w	1414w	$\delta(\text{CH})$ epoxy?
3098w			1385	1385vw	$\delta_{\text{s}}(\text{CH}_3)$ gem-dimethyl
	3067s	$\nu(\phi\text{-H})$	1363	1360vw	"
3057		$\nu_{\text{as}}(\text{CH}_2)$ epoxy	1347	1348	$\delta(\text{CH})$ epoxy
3038		$\nu(\phi\text{-H})$	1312sh	1310sh	
	3006	$\nu(\phi\text{-H})$	1298	1298	$\nu(\text{C-O}) + \nu(\text{C-C}) ?$
2998sh		$\nu_{\text{s}}(\text{CH}_2)$ epoxy		1261	epoxy ring ?
2968	2969	$\nu_{\text{as}}(\text{CH}_3)+$		1254	epoxy ring ?
		$\nu_{\text{as}}(\text{OCH}_2) ?$	1248s		$\nu(\phi\text{-O})$
2929	2927	$\nu(\text{CH})$ epoxy ?	1230sh	1231	$\delta(\phi\text{-H})$ in-plane
	2910		1185	1187	$\delta(\phi\text{-H})$ in-plane
~2890sh			1157w	1154	ϕ
2874	2871	$\nu_{\text{s}}(\text{CH}_3)$	1133	1134	
2836	2833w	$\nu_{\text{s}}(\text{OCH}_2)$	1120w		
2805vw				1113s	
2756vw	2755w		1108		
	2710w		1086	1087	$\delta(\phi\text{-H})$ in-plane
~2064w		ϕ , disubstituted	1076sh		
1891w		"		1055w	
~1766w		"	1036	1040w	$\nu_{\text{s}}(\phi\text{-O-C})$
1608	1607s	$\nu(\text{C}=\text{C}) \phi$	1012	1015w	$\delta(\phi\text{-H})$ in-plane
1583	1583	"		992w	
1511s	1510w	"	971		
	1481w	$\delta(\text{CH}_2)$ epoxy	936w	938	$\delta(\phi\text{-H})$ out-of-plane
1470sh			916	917	epoxy ring

TABLE 1(a) continued

IR	RAMAN	ASSIGNMENT
~906sh		
863	863	epoxy ring
	836	
831		$\delta(\phi-H)$ out-of-plane
	824s	$\delta(\phi)$ out-of-plane
808sh	809	
772		
	765	
758		
737w	737	
727w		
	677sh	
	667	
	654	
	650	
639w		
604w		
586w		
575	580w	
557		
504w	498w	
450	455w	
	395	$\delta(\phi)$ out-of-plane
	374sh	
	350w	
	318w	
	277sh	
	240	
	213sh	
	175w	

s = strong
w = weak
vw = very weak

sh = shoulder
v = stretching
 δ = deformation

TABLE 1(b)

INFRARED AND RAMAN BAND ASSIGNMENTS FOR NADIC METHYL ANHYDRIDE

IR	RAMAN	ASSIGNMENT	IR	RAMAN	ASSIGNMENT
	3077		1267w		
3072vw			1256vw		
3058w	3060			1246w	
3018sh		$\nu(\text{C-H})$	~ 1240		
	2993		1228s	1230w	$\nu(\text{C-O})$
2981	2985s	$\nu_{\text{as}}(\text{CH}_3)$	1216		
2945		$\nu_{\text{as}}(\text{CH}_2)$	1194w		
	2924	$\nu(\text{CH})$ tertiary ?	1180vw		
2917	2916	$\nu_{\text{s}}(\text{CH}_3)$	1137w	1141	
2879	2882	$\nu_{\text{s}}(\text{CH}_2)$	1124vw	1125	
2857sh	2857		1106w	1107	
2828vw			1083s		anhydride ring
	2744w			1074w	
1858s	1859	$\nu_{\text{s}}(\text{C=O})$	1053w	1054w	
	1852		1039w		
$\sim 1820?$	1834?		1015w	1017w	
1780vs	1781	$\nu_{\text{as}}(\text{C=O})$	1003vw	1006w	
1704w			990vw	989	
1626w	1627s	$\nu(\text{C=C})$		970w	
	1576		943s		anhydride ring
1465w	1465sh	$\delta(\text{CH}_2)$	929	934s	"
1445	1449	$\delta_{\text{as}}(\text{CH}_3)$	916s	920	"
1382w	1381	$\delta_{\text{s}}(\text{CH}_3)$	899s	902	"
1345vw		$\delta(\text{CH})$	868w	870w	"
1326w	1329w	$\delta(\text{CH})$ in-plane	853vw		
1312vw			843	844w	
1299			816sh	819	
1289	1290w		798	799w	$\delta(\text{=CH})$ out-of-plane
1277vw			786sh		

continued...

TABLE 1(b) continued

IR	RAMAN	ASSIGNMENT	IR	RAMAN	ASSIGNMENT
764sh				330w	
758w	759w			242w	
736w				211w	
712	717w			188v	
696w				154w	
673sh	672				
649sh					
635w					
622	622s				
	599				
589w					
573w	576w				
536w	539w				
506vw					
495w	498w				
461w	465w				
447w					
431w	434w				
	427w				
419vw					
408vw	412sh				
	376w				
	360w				

vs = very strong
 s = strong
 v = weak
 vw = very weak
 sh = shoulder
 v = stretching
 δ = deformation

TABLE 1 (c)

INFRARED SPECTRAL CHANGES DURING THE CROSSLINKING OF A
 STOICHIOMETRIC NADIC METHYL ANHYDRIDE/EPON 828
 MIXTURE CATALYZED BY 2.0% WEIGHT BENZYL DIMETHYLAMINE

<u>INTENSITY DECREASE</u>	<u>ASSIGNMENT</u>	<u>INTENSITY INCREASE</u>	<u>ASSIGNMENT</u>
~3060	$\nu_{as}(\text{CH}_2)$ epoxy		
3010	$\nu_s(\text{CH}_2)$ epoxy		
		2963	$\nu_{as}(\text{CH}_2)$
		~2904	$\nu(\text{CH})$
		2863	$\nu_s(\text{CH}_2)$
1858	$\nu_s(\text{C=O})$ anhydride		
1780	$\nu_{as}(\text{C=O})$ anhydride		
		1743	$\nu(\text{C=O})$ ester
		1454	$\delta(\text{CH}_2)$
		1398	$\omega(\text{CH}_2)$
		1361	
		1332	
		1267	$\nu(\text{C-O}) + (\text{C-C})$
1228	$\nu(\text{C-O})$ anhydride		
		1178	$\nu(\text{C-O})$ ester
		1155	$\nu(\text{C-O})$ ester
		1127	$\nu(\text{C-C})?$ ester
		1112	
1083	anhydride ring		
		1056	
		1012	
942	anhydride		
928	"		
915	anhydride+epoxy ring		
898	anhydride		
865	anhydride+epoxy ring?		
842			
798			
713			
		ν = stretching	
		δ = deformation	
		ω = wagging	

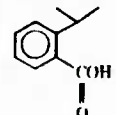
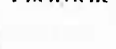
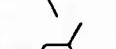
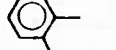
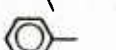
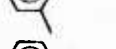
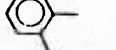
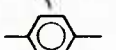
TABLE II.

Tentative Infrared Absorption Assignments for the Three Cured Epoxy Resins and the Absorption Variations During Degradation

Wavenumber (cm ⁻¹)	DGEBA				DGEPP				DGEHF				Functional group	Vibration mode
	IR ^a	TD ^b	TO ^c	PO ^d	IR	TD	TO	PO	IR	TD	TO	PO		
3570	x ^e								x				} R-OH	$\nu(\text{O-H})$
3550					x									
3525		+ ^f	+			+	+				+		} $\begin{array}{c} \text{O} \\ \\ \text{ArCOH} \end{array}$	$\nu(\text{O-H})$
3430						+	+							
3350								+				+	} Ar-OOH	$\nu(\text{O-H})$
3300				+										
3200												+	} Methyl	$\nu(\text{C-H})$
3068					x	-	-	-						
3060									x	-	-	-	} Methylene	$\nu(\text{C-H})$
3052	x	- ^g	-	-										
3038					x	-	-	-					} Methyl	$\nu(\text{C-H})$
3034	x	-	-	-					x	-	-	-		
2970	x	-	-	-									} Methylene	$\nu(\text{C-H})$
2935	x	-	-	-										
2933					x	-	-	-					} Methylene	$\nu(\text{C-H})$
2930									x	-	-	-		
2880					x	-	-	-					} Methylene	$\nu(\text{C-H})$
2876	x	-	-	-					x	-	-	-		
1808		+	+	+		+	+			+	+	+	} $\begin{array}{c} \text{O} \quad \text{O} \\ \quad \\ \text{R}^1-\text{O}-\text{C}-\text{C}-\text{R}^2 \\ \\ \text{H} \end{array}$	$\nu(\text{C=O})$
1790							+							
1784			+	+							+	+	} Lactone	$\nu(\text{C-O})$
1782					x	-	-	-						
1775							-						} Lactone	$\nu(\text{C-O})$

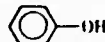
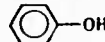
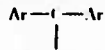
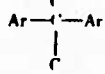
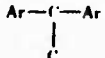
continued...

TABLE II (continued)

1765	x	+	+	+		+			x	+	+	+	$\begin{array}{c} \text{Y} \\ \\ \text{R} \text{---} \text{C} \text{---} \text{O} \text{---} \text{R} \\ \\ \text{O} \\ \text{Lactone} \end{array}$	}	$\nu(\text{C}=\text{O})$			
1751					x	-	-									$\begin{array}{c} \text{O} \\ \\ \text{R} \text{---} \text{C} \text{---} \text{O} \text{---} \text{R} \\ \text{RCHO} \end{array}$	}	
1745		+	+	+						+	+							
1732	x	+	+	+				x		+	+						}	
1725						+	+	+							}			
1715	x	+	+	+	x	+	+	+	x	+	+	+	$\begin{array}{c} \text{O} \\ \\ \text{R} \text{---} \text{C} \text{---} \text{O} \text{---} \text{H} \\ \text{Phenoxy} \end{array}$			}	Quadrant stretching	
1665		+	+	+		+	+	+			+	+			}			
1610	x	-	-	-	x	-	-	-	x	-	-	-				}		
1578	x	-	-	-	x	-	-	-	x	-	-	-			}			
1510	x	-	-	-	x	-	-	-	x	-	-	-				}		
1505												+			}			
1480		+	+	+							+					}		
1465					x	-	-	-							}			Semicircle stretching
1448									x	-	-	-				}		
1440						+		+							}			
1425		+	+							+	+	+				}		
1412	x	-	-	-	x	-	-	-	x	-	-	-			}			

continued...

TABLE II (continued)

Wavenumber (cm ⁻¹)	DGEBA				DGEPP				DGERF				Functional group	Vibration mode
	IR ^a	TD ^b	TO ^c	PO ^d	IR	TD	TO	PO	IR	TD	TO	PO		
1288					x	-	-	-					Lactone Ester or acid	$\nu(\text{C}-\text{O}-\text{C})$
1286						+	-	+						$\nu(\text{C}-\text{O}-\text{C})$ or $\nu(\text{C}-\text{O})$
1280			+	+				+			+	+		$\nu(\text{C}-\text{O})$
1280			+	+				+			+	+		$\nu(\text{C}-\text{O})$
1255	x	-	-	-	x	-	-	-	x	-	-	-	Ar-O-R	$\nu(\text{C}-\text{O}-\text{C})$
1245				+				+				+	Ar-OH	$\nu(\text{C}-\text{O}-\text{C})$
1202				-				-			-	-		$\nu(\text{C}-\text{C})$
1184	x	-	-	-	x	-	-	-						$\nu(\text{C}-\text{C})$
1180									x	-	-	-		
1170				+		+		+		+	+	+		$\nu(\text{C}-\text{C})$
1120	x	-	-	-	x	-	-	-	x	-	-	-	Aliphatic chain	$\nu(\text{C}-\text{C})$
1096									x	-	-	-	Aliphatic ether	$\nu(\text{C}-\text{O}-\text{C})$
1086					x	-	-	-						
1035	x	-	-	-	x	-	-	-	x	-	-	-		
1015					x	-	-	-	x	-	-	-		
1010	x	-	-	-									Lactone	$\nu(\text{C}-\text{O}-\text{C})$
965					x	-	-	-						
940					x	-	-	-						
925					x	-	-	-						
890							+	+					Peroxide	$\nu(\text{O}-\text{O})$
885		+	+	+							+	+		

continued...

epoxide absorbance caused by differences in specimen thickness can be eliminated by normalizing the epoxide peak height to an internal reference peak which appears at 1510 cm⁻¹ due to the phenyl groups.

$$f_{915} = \frac{A_{915,t}}{A_{1510,t}} \times \frac{A_{1510,0}}{A_{915,0}}$$

f_{915} = fraction unreacted epoxide at time t

$A_{915,t}$ = specimen absorbance at 915 cm⁻¹ due to epoxide at time t

$A_{1510,t}$ = specimen absorbance at 1510 cm⁻¹ at time t

$A_{915,0}$ = initial absorbance at 915 cm⁻¹

$A_{1510,0}$ = initial absorbance at 1510 cm⁻¹

Dannenbergs(50) used near IR to study the curing reaction of epoxy resins, and demonstrated the advantages of this technique which is very sensitive due to the fact that epoxide group has a strong overtone absorption frequency in the near IR region. Several studies(48-50,7,8) have been reported on the epoxy curing process by FTIR. Appropriate programs for data processing are available and easily modified to any specific reaction needs. These techniques have been found very helpful to interpret the complicated crosslinking reaction of epoxy resins. Sprouse, Halpin, Sacher(54) used FTIR spectroscopy to measure the extent of cure in fiber-reinforced-epoxy composites by two different techniques. The two sampling techniques are : (1) thin films of neat resin held between salt plates and (2) internal reflectance spectroscopy. Thin films were cured in the same program as used in the corresponding composite fabrication. IR spectra were recorded at short time intervals throughout the cure cycle. Internal reflectance measurements were performed on the corresponding composites and results were compared with thin film measurements. Antoon and Koenig(55) demonstrated the utility of FT-IR difference spectra for investigating the composition of neat epoxy resin, hardener, and catalyst as well as the composition and degree of crosslinking of the cured matrices. Improved

precision is achieved by using a least-squares curve-fitting program for the determination of the composition of the uncured and cured epoxy matrices mixtures.

8.0 QUALITY CONTROL OF EPOXY MATRICES IN FIBER--REINFORCED COMPOSITES

Fiber reinforced composite structure have gained a significant position as materials of construction for the aerospace industry and transportation industry. It thus follows that large expenditures of funds and human lives are dependent on the reliability of these products. An important step in gaining confidence in a product is knowing that the starting prepreg has the same chemical formulation, and each lot of material has been processed in the same manner.

Antoon and Koenig(56) developed a general and convenient method for determining simultaneously the initial resin composition and the extent of crosslinking of epoxy matrices. This technique can be used as a quality control method to determine that the starting prepreg has the same chemical formulations and that each lot has been processed in the same manner.

Figure 9 shows the results of the factor analysis of crosslinked epoxy/anhydride resins in the 2000-1400 cm^{-1} region. The plot of logeigenvalue in descending order reveals a break in the eigenvalue magnitude between the third and fourth eigenvalue. As indicated by Antoon and Koenig, the number of these larger eigenvalues is equal to the number of components in the system. Therefore, the spectrum of the crosslinked epoxy matrix may be approximated by a linear combination of only three linearly independent component spectra. The three spectra chosen to represent the components were that of pure NMA, pure Epon 828, and a difference spectrum characteristic of the crosslinking reaction. The difference spectrum was calculated by subtracting the spectrum of a stoichiometric mixture of NMA and EPON 828 crosslinked for 37 min at 80°C from the spectrum of the same reactant mixture crosslinked for 83 minutes at 80°C . The procedure is illustrated in Figure 10. Figure 11 shows the absorbance spectra employed for the analysis of the crosslinked epoxy matrix. A boxcar function is included as a fourth component in the least-squares

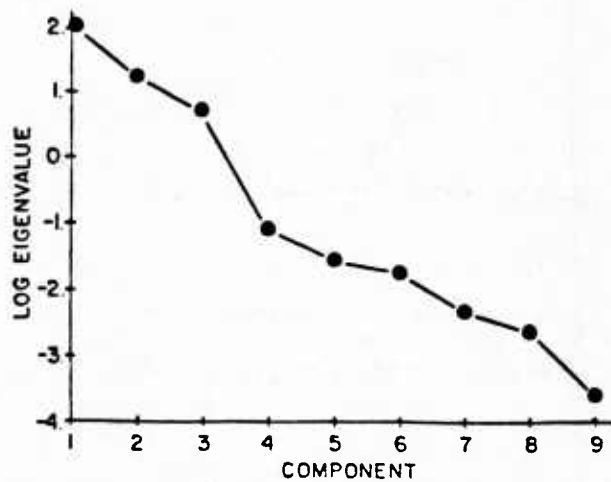


Figure 9. Factor analysis of crosslinked epoxy/epoxide resin in the 2000-1400 cm^{-1} region. Tertiary amine-catalyzed reactions.

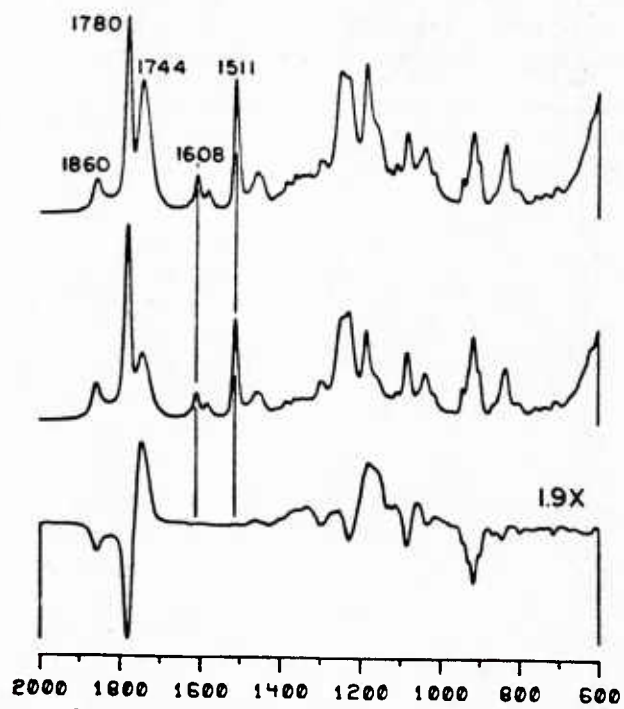


Figure 10. Generation of difference spectrum characteristic of 80°C crosslinking of stoichiometric mixture of NMA/EPON 828. Top: crosslinked 83 min. Middle: crosslinked 37 min. Bottom: difference spectrum (top minus bottom)

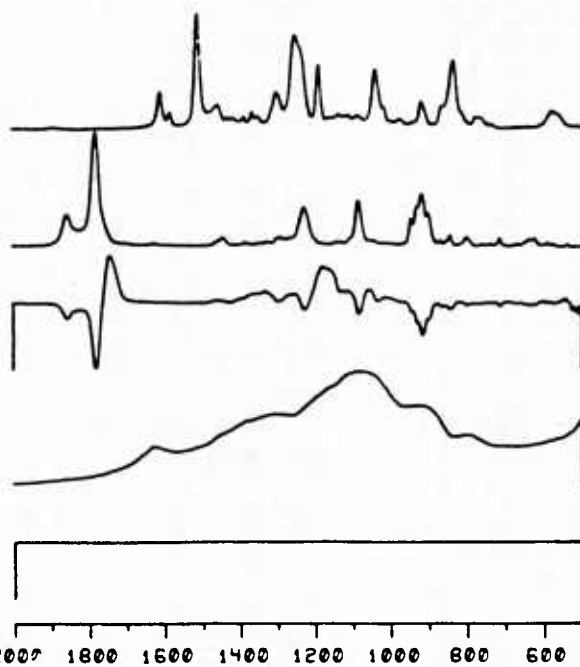


Figure 11. Spectral components in a crosslinked epoxy/anhydride (polyester matrix filled with S-glass. From top: EPON 828 epoxy resin, nadic methyl anhydride, crosslinking difference spectrum (from Fig. 2), S-glass, and boxcar function.

analysis of the resin in order to prevent errors in the background level from affecting the accuracy of the least-squares coefficients. The spectrum of S-glass, also shown in Figure 11, is included as a fifth component in the least-squares curve-fit analysis for S-glass reinforced composites. After performing the least square curve fitting, the quality of the fit between the experimental resin spectrum and the least-squares fitted spectrum is illustrated in Figure 12. The least square coefficient corresponding to the difference spectrum is a measure of the extent of crosslinking, and the coefficients corresponding to the pure NMA and pure epoxy are a measure of the amount of reactants.

Figure 13 shows the factor analysis of glass fiber-reinforced epoxy composite. Since there is no obvious separation between the nonzero and error eigenvalues, it is an arbitrary decision to determine the number of components that contribute to the composite spectrum. Antoon and Koenig attribute this problem to systematic errors in the spectra themselves. Figure 14 shows a least-square curve fitting of five component spectra to the spectrum of a composite. As can be seen, the fitted curve and the experimental result coincide satisfactorily. The results for nonreinforced matrices consisting of stoichiometric mixtures of epoxy and anhydride crosslinked to various extents are given in Table 3. The weight percent compositions are derived from the least-squares coefficients after scaling the EPON 828 and NMA spectra. The actual weight percent compositions are from weighing. As indicated by the calculated standard errors, the accuracy is generally within 2 percent and most notably the accuracy is retained even at very high extents of crosslinking. Table 4 shows the least-squares analysis of S-glass reinforced crosslinked epoxy matrix.

The least-squares analysis of epoxy matrix yields reproducible information with an accuracy limited by several spectroscopic problems. A source of error comes from sample preparation limitations. The wedge effect occurs from nonuniformity in the infrared pathlength through the sample, that result in the deviation from Beer law and causes a weakening of the stronger absorption bands in highly-absorbing materials. Another source of inaccuracy is due to the change in the spectra of NMA and EPON 828 when the molecules are in electronic environments that differ from that of pure liquids. Finally, since the

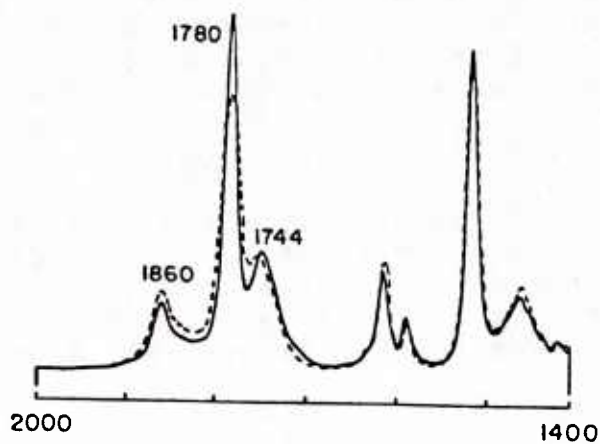


Figure 12. Least-squares fit of the spectra EPON 828 and Nadic methyl anhydride, the crosslinking difference spectrum and the boxcar function to the spectrum of a partially crosslinked polyester matrix. Solid line: experimental matrix spectrum and dotted line: fitted spectrum.

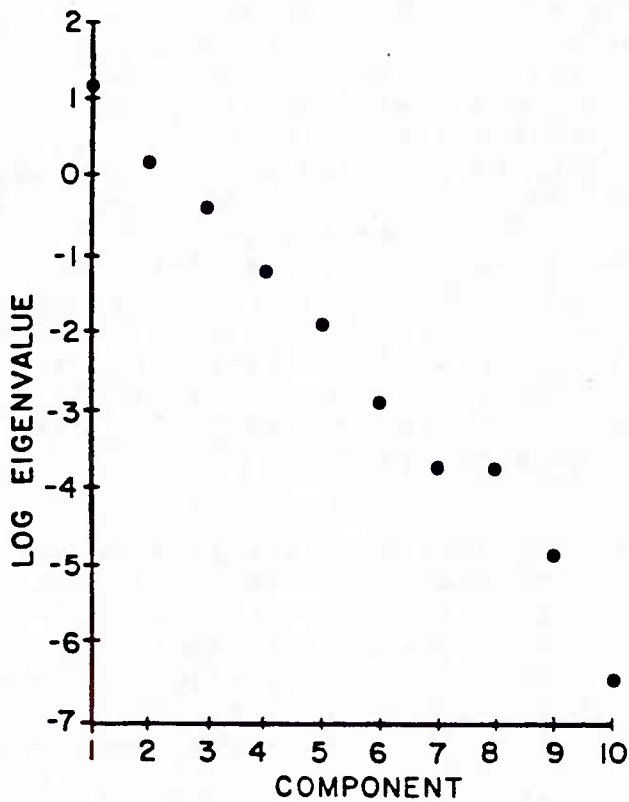


Figure 13. Factor analysis of the spectra of crosslinked polyester composites in the 1550-650 cm^{-1} region.

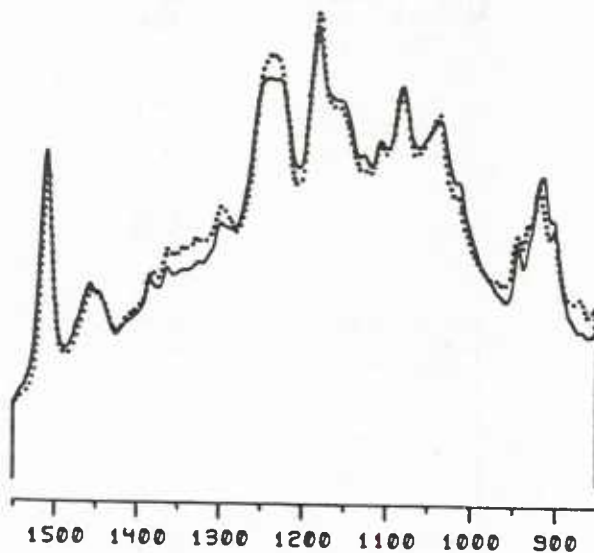


Figure 14. *Least-squares fit of five component spectra (from Fig. 3) to the spectrum of a composite in the 1550-850 cm⁻¹ region.*

Table 3 Least-Squares Analysis 2000-1400 cm^{-1} of 1:1 Stoichiometry Anhydride:Epoxy Mixtures (0.5% wt BDMA Catalyst) Crosslinked at 90°C

Uncured	Least-squares calculation (%)	Composition by weighing	Extent crosslinked from I(1860)/I(1608)
EPON 828	51.99 ± 1.89 (wt%)	50.77	0.0
NMA	48.01 ± 0.96 (wt%)	49.23	
Extent crosslinked	-1.65 ± 1.37		
30 min @ 90°C			6.6
EPON 828	52.06 ± 1.97	50.77	
NMA	47.94 ± 1.00	49.23	
Extent crosslinked	5.97 ± 1.42		
60 min @ 90°C			13.2
EPON 828	51.62 ± 2.11	50.77	
NMA	48.38 ± 1.07	49.23	
Extent crosslinked	12.42 ± 1.51		
90 Min @ 90°C			18.8
EPON 828	51.58 ± 2.24	50.77	
NMA	48.42 ± 1.14	49.23	
Extent crosslinked	18.47 ± 1.60		
120 min @ 90°C			31.0
EPON 828	51.11 ± 2.31	50.77	
NMA	48.89 ± 1.17	49.23	
Extent crosslinked	28.14 ± 1.64		
6 hr @ 90°C			70.2
EPON 828	51.99 ± 1.89	50.77	
NMA	48.01 ± 0.96	49.23	
Extent crosslinked	65.35 ± 1.36		

Table 4 Least-Squares Analysis of S-Glass Reinforced Crosslinked Epoxy Matrix

Temp., time of curing	E(predicted)	Region			
		2000-1400 cm^{-1}		1550-850 cm^{-1}	
		R	E	R	E
80°C, 70 min	31.1	1.2	51	0.93	54
80°C, 90 min	39.3	1.1	59	0.88	55
80°C, 110 min	47.5	1.1	57	0.90	59
80°C, 130 min	55.6	1.0	62	0.92	62
80°C, 180 min	63.7	1.0	70	0.96	67
160°C, 30 min	83.5	1.0	82	0.93	80

refractive indices of KBr, crosslinked resin, and S-glass spectrum are substantially different, significant nonlinearity in spectra occurs by the scattering of the infrared beams. Although there exists some spectroscopic problem, Antoon and Koenig(56) suggest some methods of improvement. Statistical methods of determining the number of components present may be helpful. Multiple difference spectra, each representing the crosslinking at each stage, can improve the sensitivity of least square methods.

9.0 INFRARED STUDIES OF DEGRADATION OF EPOXY RESIN

Another important application of infrared spectroscopy in characterization of cured epoxy composites is to determine the effect of in-service exposure conditions (degradation, hydrolysis, weathering, aging) on composites. The surface of a glass fiber-reinforced epoxy composite is degraded rapidly upon outdoor exposure unless it is protected by a UV-absorbers or a paint. The degradation phenomena are difficult to study due to the uncertainty in epoxy resins composition and the intractable nature of the cured composite that prevent the use of conventional techniques of polymer analysis. Although DSC can be used to evaluate the thermal stability of epoxy composites, it only gives an estimate of thermal stability and can not provide enough information to interpret the degradation process. Several techniques, such as gas chromatography, chemical analysis, mass spectroscopy, have been developed to study the degradation phenomena. These methods are based on the analysis of the degradation products related to the original polymer. However, these methods are complicated, since the degradation of material at high temperature may cause rearrangement of the degradation fragments, or other reactions. Therefore, degradation product analysis may lead to a false degradation mechanism. On the other hand, FTIR can eliminate these problem. George, Sacher, and Sprouse(57) investigated the photo-protection of the surface resin of a glass fiber-reinforced composite with FTIR using a single-pass internal reflectance attachment for the surface study. As shown in Figure 15, the IR spectrum shows a strong ester carbonyl band at 1735 cm^{-1} which is used as an index of photo-oxidation under exposure to the sunlamp. This band can be used to measure the photo-oxidation rates of different epoxy resins as shown in Figure 15. The 1009 resin is a mixture of novolac epoxy and bisphenol A epoxy.

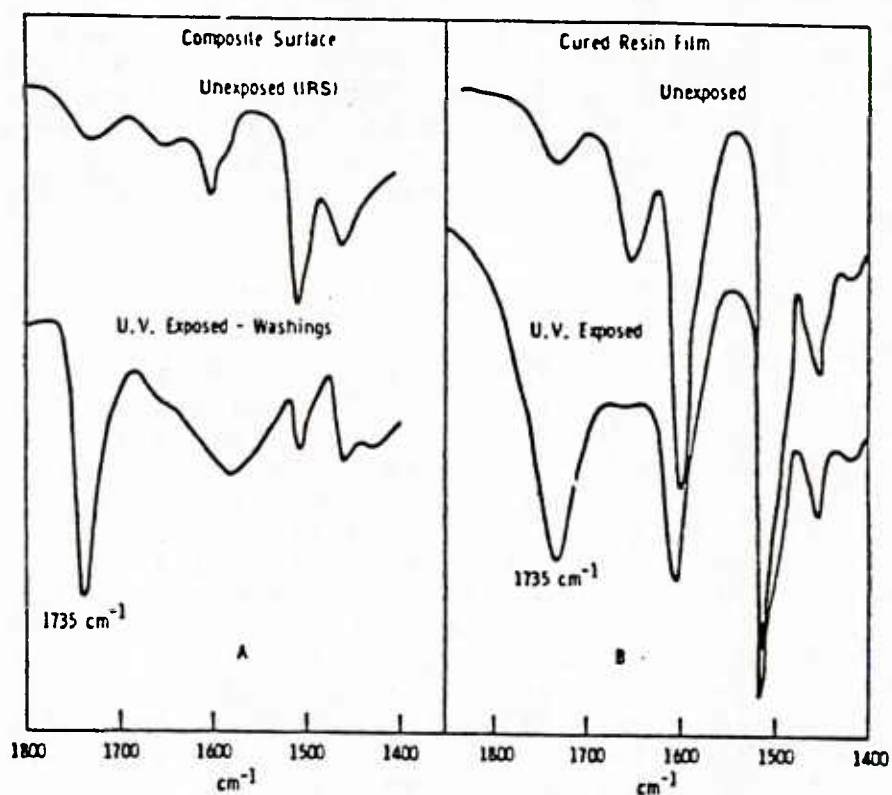


Figure 15. (a) IRS-IR spectrum of unexposed 1009-26 composite surface and transmission IR of surface washings from composite surface exposed 4000 hr to sunlamp. (b) Transmission IR of air-cured 1009 resin film before and after 55 hr of exposure to sunlamp.

Figure 16 showed the oxidation rates for different epoxy resins. The observed oxidation rate for the epoxy novolac is eight times that of the bisphenol A epoxy. The high photo-oxidation rate of the cured epoxy novolac is related to the cure process itself.

The uncured resin showed negligible absorption of solar radiation (Figure 17). When heated at 165 C for a short time, an intense absorbing chromophore is formed. If the cure is carried out under vacuum, chromophore formation can be minimized. It was found that novolac epoxy shows the chromophore formation which justify the reason why the photo-oxidation rate of the novolac epoxy is higher. On the other hand from the changes in the IR spectrum during cure, it was found that there occurs a strong carbonyl group absorption that is due to oxidation, and this absorption does not occur if the cure is under vacuum. Therefore, the weathering stability of an epoxy resin can be affected by the conditions of cure.

Pearce used the subtraction of absorbance spectra to compare the functional group stability of epoxy resin. Figure 18 shows the IR spectra and difference spectra of cured DGEBA, before and after thermal degradation. The absorption bands of the cured resin have decreased in intensity and new bands have appeared. To understand the relative stability of the functional groups in the resin, as shown in Figure 19, for DGEBA, the subtracted spectra were obtained by changing the k parameter. After the band at 830 cm^{-1} (p-phenylene) is canceled ($A_{830} = 0$) it shows that the difference absorbance A_{3052} , A_{3034} , A_{2970} , A_{2935} and A_{2876} change from negative to positive. These changes indicate that the p-phenylene group is not as stable as the $-\text{CH}_3$ and $-\text{CH}_2$ groups and may rearrange to a more stable form of substituted benzene species. After canceling the $-\text{CH}_3$ group absorption, the C-H stretching frequencies almost disappear while those of the $-\text{CH}_2$ group show negative difference absorbances. The result indicates that the $-\text{CH}$ group has similar stability to the benzene ring and higher stability than the $-\text{CH}$ -group. Repeating this method, Pearce established the order of functional group stability as total methyl group \sim total benzene group $>$ methylene $>$ P-phenylene $>$ ether linkage $>$ isopropylidene. Based on FTIR analysis, it is proposed that initially the isopropylidene group degrades, releasing the first methyl group and retaining the second methyl group until the latter stages of degradation. The p-phenylene group undergoes a Claisen rearrangement and forms a 1,2,4-trisubstituted benzene. Other possible initial degradation steps are proposed. The

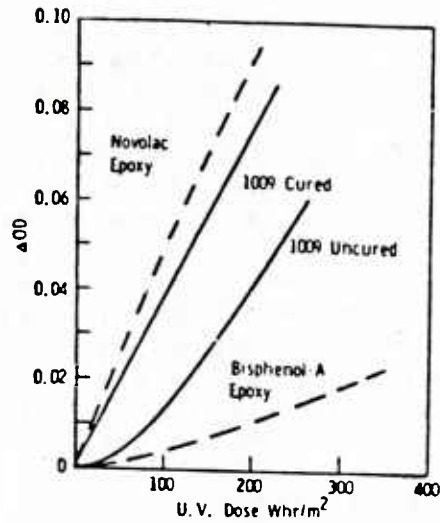


Figure 16. Change in aliphatic carbonyl concentration measured by absorption intensity at 1735 cm^{-1} (ΔOD) with total UV dose from 300 to 350 nm for the resin systems indicated.

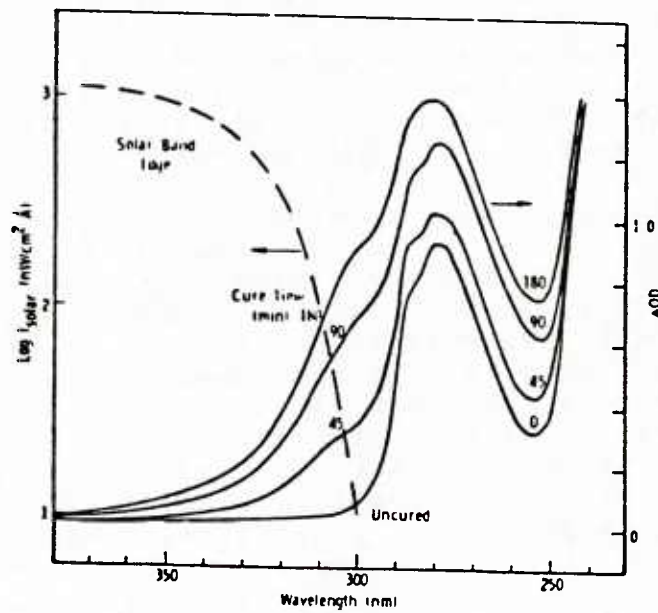


Figure 17. Changes in the UV absorption spectrum of $1.5\text{-}\mu\text{m}$ film of 1009 resin during cure in air at 165°C for the times shown. The reported solar spectrum in this region is also shown.

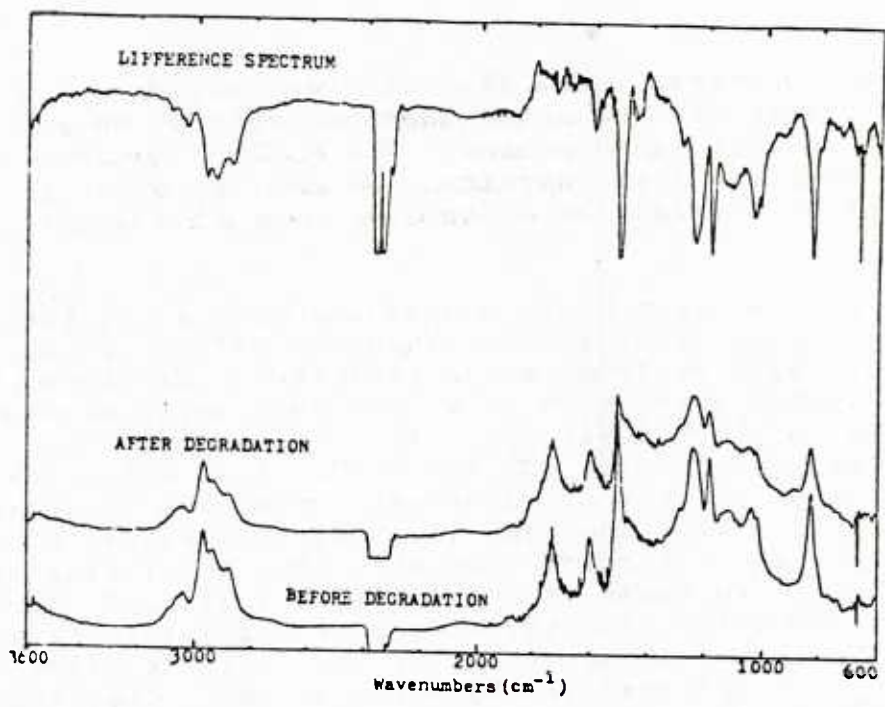


Figure 18. IR and difference spectra of cured DGEBA before and after thermal degradation at 300°C

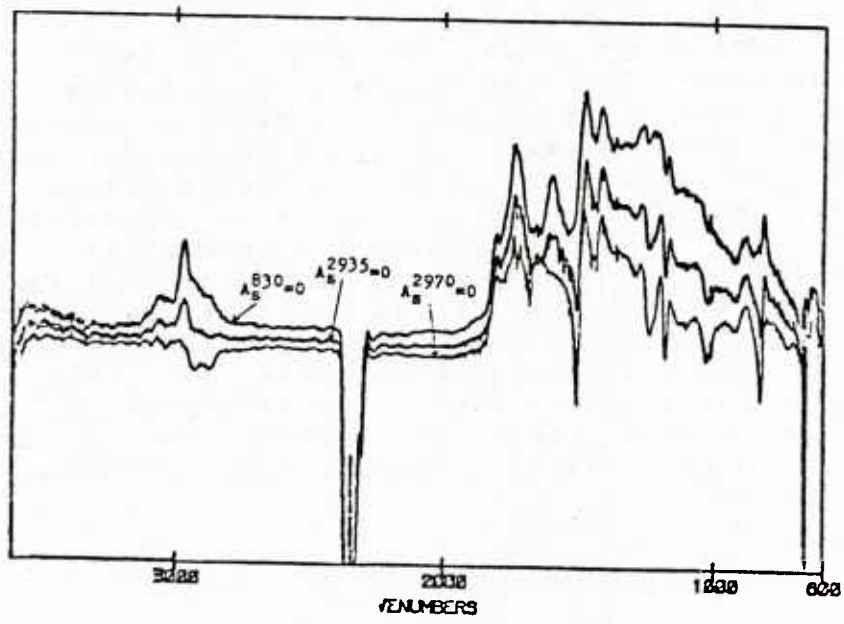


Figure 19. Variations in the thermal degradation difference spectrum of cured DGEBA during canceling process.

oxidative, thermal, and photodegradations were found to be related to the autooxidative degradation processes for aliphatic hydrocarbons. The Wieland rearrangement and Norrish type reactions, as well as other possible oxidation degradation mechanism, were also suggested.

On the other hand, Antoon and Koenig utilized FTIR to identify irreversible chemical effects of moisture on an anhydride-cured epoxy resin(58). Exposure of a crosslinked epoxy film to 80°C liquid water environment caused a hydrolysis of the unreacted anhydride groups(approximately 5% of the initial anhydrides) to diacids. This effect, dominant during the early stages of moisture exposure, is illustrated in Figure 20. The decrease in anhydride concentration is indicated by intensity decrease of NMA vibrations at 1860, 1080 cm^{-1} . Figure 20 also shows the effect of long-term exposure of the same epoxy film to 80°C liquid water. The short-term effect is hydrolysis and leaching of unreacted NMA molecules; the longer-term effect rule out matrix hydrolysis and may be due to subtle structural changes such as perfection of the H bonding of polar groups.

The effects of stress on moisture stability is shown in Figure 21. The intensity decrease at 1744 cm^{-1} suggests a loss of ester group; intensity increases at 3500 and 1720 cm^{-1} may be assigned to the formation of alcohol groups and carbonyl groups, respectively. Such a hydrolysis reaction, though very slow, is expected to be important in initiating irreversible matrix degradation. As shown by Antoon and Koenig, the degradation effect is slightly more rapid when the epoxy resin is under stress. In Figure 22 the relative intensity of the ester carbonyl peak at 1744 cm^{-1} is plotted versus exposure time in pH 11.9 water(80°C) for epoxy films with a range of applied tensile stress levels. High stress dramatically increases the hydrolysis rate.

10.0 RAMAN SPECTROSCOPY

Since the advent of laser, Raman Spectroscopy has become an important analytical tool in polymer research. Raman scattering occurs for those vibrational motions, which produce a polarization or distortion of the electron charge of the chemical bonds. Thus the stretching motion of a homonuclear diatomic molecule is active in the Raman effect. the

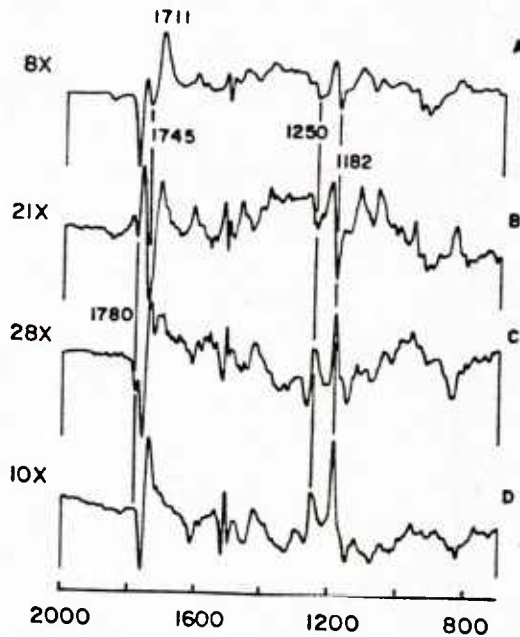


Figure 20. Difference spectra showing the progression of spectral changes occurring in epoxy resin in 80°C distilled water. Same sample as in Figure 1. (A) 4.4 days minus zero days exposure. (B) 35 days minus 12 days. (C) 50 days minus 35 days. (D) 224 days minus 98 days.

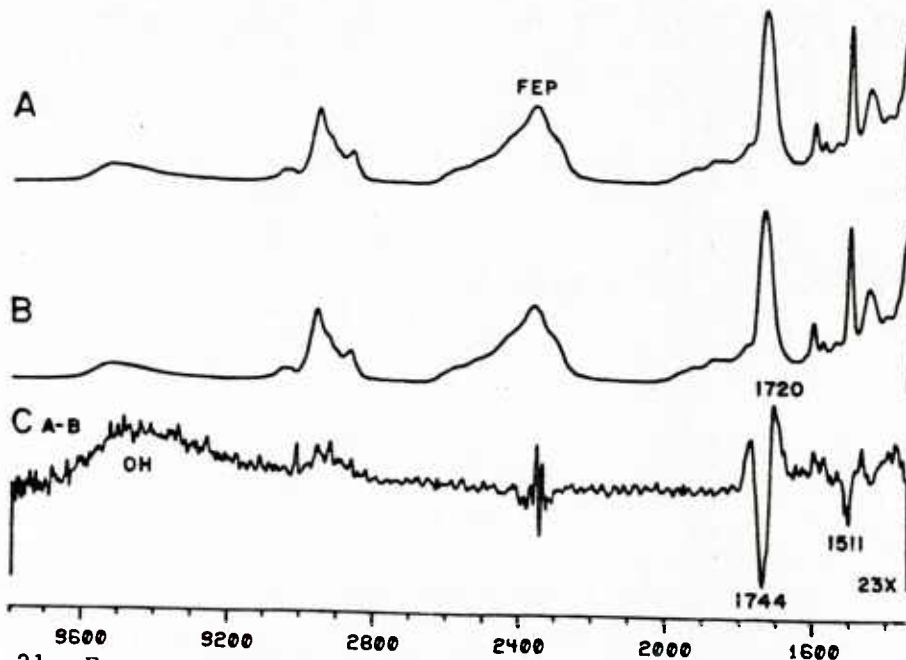


Figure 21. Exposure of epoxy resin to 100% relative humidity air at 80°C while under 2.6×10^8 dyn/cm² tensile stress. (A) Absorbance spectrum after 155 days exposure. (B) Absorbance spectrum after 71 days exposure. (C) Difference spectrum: A minus B.

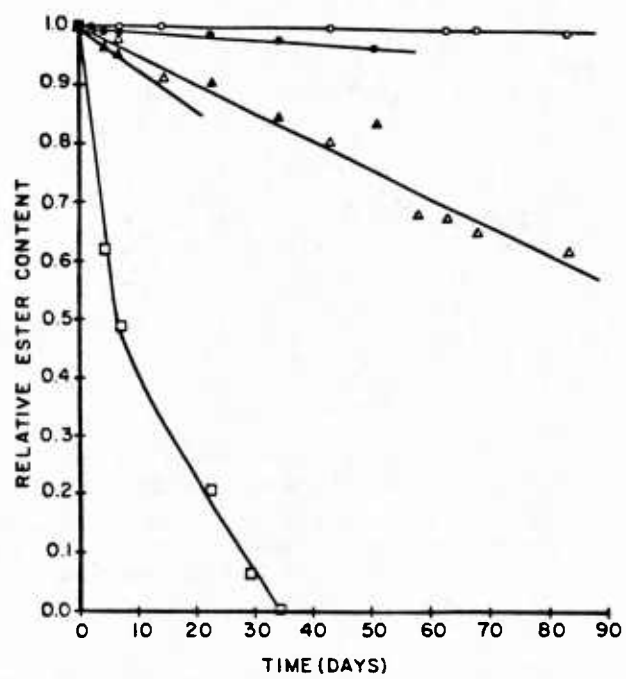


Figure 22. Relative ester content (1744 cm^{-1} intensity) versus time for epoxy resins under varying tensile loads. Environment is pH 11.9 water at 80°C . Stress ($\text{dyn}/\text{cm}^2 \times 10^{-8}$): (O) 0.0; (●) 1.9; (Δ) 2.6; (\blacktriangle) 4.0; (\square) 5.4.

Raman effect provides more information about the nonpolar portions of the molecules. While the IR effect yields information about the polar portions of the molecule. Due to the complementary nature of the two types of spectroscopy, they should both be used whenever possible. since Raman spectroscopy enhances the effectiveness of IR for solving chemical structure problems and vice versa.

Since the Raman effect is a light scattering rather than a light transmission process, the transparency, size, and shape of the samples are relatively unimportant. Thus, one can run large samples or extremely small sample samples with comparative ease in the Raman. Filled polymer, composites, present difficulty for IR investigations, since the fillers such as glass, clay, and silica are strong IR absorbers that block the IR spectrum of the polymer. These particulate fillers (glass, silica) are poor Raman scatters, so the Raman spectrum of the polymer is obtainable without removal of the filler.

Only a few of reports have appeared in the literature, Lu and Koenig(59) used the Raman spectroscopy to study the curing of epoxy resins. Strong Raman lines which are characteristic of epoxy resin and independent of the state of cure are found at 640, 823, 1114, 1188, 1232, and 1608 cm^{-1} , which are due to the bisphenol A skeleton. The epoxy group has lines at 768, 809, 1156 cm^{-1} , which are sensitive to the degree of crosslinking.

11.0 DIELECTRIC ANALYSIS

The dielectric analysis is based on measuring the ability of the dipole in a system to align with an oscillating electric field. In aligning the dipoles, a certain amount of energy is utilized. By subjecting an epoxy system to the oscillating field, information about the viscous and elastic properties can be obtained through the following relationships:

$$E = E_0 \exp i\omega t$$

$$D = D_0 \exp (i\omega t + \delta)$$

where E is the amplitude of the electric field and D is the displacement. Furthermore, we have

$\bar{D} = \bar{E} \times \bar{F}$, where \bar{E} is the complex dielectric constant and is equivalent to $(E' - iE'')$, the real and imaginary components.

The ratio $E''/E' = \tan\theta$ is called the loss factor and is related to the well known G''/G' relationships for viscoelastic materials. The dielectric spectrometer is capable of giving a direct measurement of the dissipation or loss factor for epoxy resin when subjected to an alternating electric field. Hence, changes in the flow characteristics are discernible by this method. The degrees of freedom of the dipoles are indicative of the viscous properties of a material. A typical dielectric analysis is shown in Figure 23, where capacitance, dissipation factor, and temperature are plotted as a function of time.

The dissipation factor curve is related to the curing of the epoxy matrix. The lefthand peak of the curve corresponds to the softening and flow of the resin system. The righthand peak is associated with the setting of the matrix. The portion between the peaks shows low dissipation since the epoxy resin displays a less viscous behavior. This is the region where process changes such as the application of pressure for consolidation of the laminates are performed.

Examples of the use of dielectrometry in the study of composites have been reported in the literature. Sanjana and Rosenblatt(60) demonstrate the feasibility of using dielectric analysis as a means of monitoring and controlling cure of epoxy composites in autoclave molding. The mechanical properties are correlated with the variables on the dissipation factor profiles.

Another method related to dielectric changes when an epoxy cures is an electric monitoring technique(61) based on the charge-flow transistor, which resembles a conventional metal-oxide-semiconductor-field-effect transistor, but with a portion of the metal gate replaced by the epoxy resin under study. The dramatic change in the shape of the electrical signal during cure can be related to corresponding changes in both the real and imaginary parts of the dielectric constant and can be used for monitoring curing. A typical signal output is shown in Figure 24:

The instrumentation in dielectric analysis is simple, and since the peaks in the curve which result from relaxation phenomena, associated with softening and gelation of epoxy resin are frequency dependent, these peaks do not define the point in time when softening or gelation occur. Therefore, it should be careful to interpret the dielectric analysis.

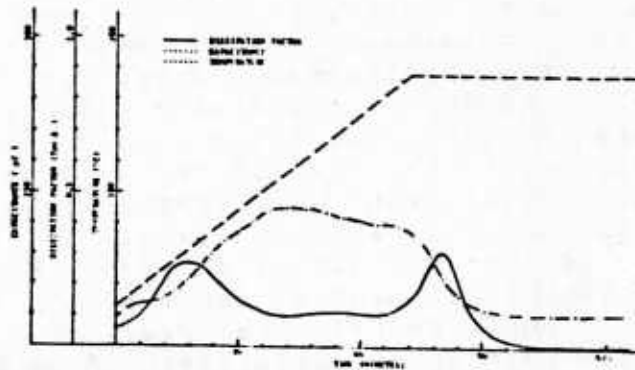


Figure 23. Dielectric analysis of 350°F epoxy prepreg.

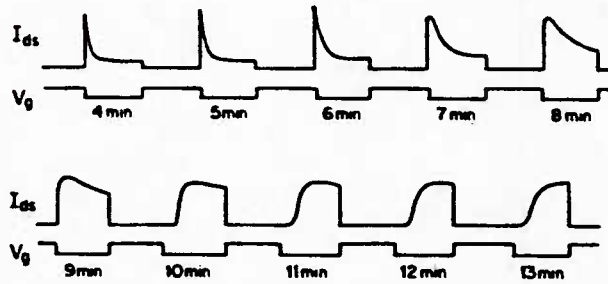


Figure 24. CFT drain current waveforms (I_{ds}) during cure of a commercial 5-minute epoxy at room temperature (3).

12.0 CONCLUSION

Several methods are reviewed in this paper for characterizing the epoxy matrix in glass fiber-reinforced composites. TBA and dielectric analysis yield the rheological changes during curing that are useful in composite processing. DSC gives the extent of cure on the assumption that the extent of cure is proportional to the heat of reaction but this assumption is invalid for complicated crosslinking reaction. IR spectroscopy is very useful in studying the mechanism of cure and extent of cure. FTIR is an ideal tool for investigating the degradation behavior of composites, and control the quality of epoxy matrices in fiber-reinforced composites. A combination of these techniques will become a powerful method in the study of composites.

13.0 ACKNOWLEDGEMENT

This research and overview report was funded by the Army Materials and Mechanics Research Center (AMMRC) as a subtask in an Army Research Office Grant No. DAAG29-81-D-0100 entitled "Quality Control and Non-destructive Evaluation Techniques for Composites - Part II: Physiochemical Characterization Techniques - A State-of-the-art Review". The author wishes to gratefully acknowledge helpful consultations with Dr. Richard Shuford of AMMRC during the preparation of this overview.

14.0 REFERENCES

1. Samuel S. Oleesky and J. Gilbert Mohr, Handbook of Reinforced Plastics, The Soc. of the Plast. Ind., Inc., 1978, p. 71.
2. Henry Lee, Kris Neville, Handbook of Epoxy Resins, McGraw-Hill Book Company, 1967, pp. 13-1.
3. L.H. Tateosian and J.R. Royer, "Effect of Mixing Efficiency on Epoxy Properties", presented at the 15th ACS Middle Atlantic Regional Meeting, Jan. 7, 1981, Washington, D.C.
4. J.P. Bell, "Epoxy Resin: Effect of Extent of Mixing on Properties", J. of Appl. Polym. Sci., 27 3503, 1982.
5. T.T. Chiao, and R.L. Moore, "A Room-Temperature-Curable Epoxy for Advanced Fiber Composites". Proceedings of the 29th Annual Technical Conference on Reinforced Plastics/Composites Institute, SPI, 1974, Sec. 16-B.
6. S.L. Kaplan, A. Katjakian, E.L. Mitch, "Fast Curing Acid/Epoxy-Anhydride/Epoxy Resins". Proceedings of the 30th Annual Technical Conference on Reinforced Plastics/Composites Institute, SPI, 1975, Sec. 8-C.
7. L. Buckley, D. Roylance, "Kinetics of a Sterically Hindered Amine Cured Epoxy Resin System", Polym. Eng. Sci., 22(3), 166, (1982).
8. T. Donnellan, D. Roylance, "The Curing of a Bisphenol A-type Epoxy Resin", Polym. Eng. Sci., 22(13), 821 (1982).
9. J.C. Spitsbergen, P. Loenwrigkeit, C. Bluzstein, J. Sugarman, and W.L. Lauze, "Improved Epoxy Resin from Dihydroxy-diphenyl Sulfone", Proceedings of the 26th Annual Technical Conference on Reinforced Plastics/Composites Institute, SPI, 1971, Sec. 19-C.
10. S.L. Kaplan, E.L. Mitch, and A. Katzakian, "Epoxy/Imide Resin Systems", Proceedings of the 30th Annual Technical Conference on Reinforced Plastics/Composites Institute, SPI, 1975, Sec. 19-A.
11. E.H. Catsiff, H.B. Dee and R. Seltzer, "Hydantoin Epoxy Resins as Matrix Components", Proceedings of the 33rd Annual Technical Conference on Reinforced Plastics/Composites Institute, SPI, 1978 Sec. 16-C.
12. C.J. Busso, H.A. Newey, T.D. Buckman, and H.V. Holler, "Chemical Structure-Mechanical Properties Studies on Pure Epoxy Resin Systems", Proceedings of the 25th Annual Technical Conference on Reinforced Plastics/Composites Institute", SPI, 1970, Sec. 3-B.

13. McGarry, F.J. et. al., R69-35, MIT, July 1, 1969.
14. A.C. Soldatos and A.S. Burhans, "Cycloaliphatic Epoxy Resins with Improved Strength and Impact Coupled with High Heat Distortion Temperature", Proceedings of the 25th Annual Technical Conference on Reinforced Plastics/Composites Institute, SPI, 1970, Sec. 3-C.
15. A.R. Siebert, E.H. Rowe, C.K. Riew, and J.M. Lipiec, "Toughness vs. Flexibility in Epoxy Resins (Part A)", Proceedings of the 28th Annual Technical Conference on Reinforced Plastics/Composites Institute, SPI, 1973, Sec. 1-A.
16. H. Samejima, "Formation and Properties of Elastomer Modified Epoxy Resins", Am. Chem. Soc. Div. Polym. Chem., Polymer Preprint, 22(2), 127, 1981.
17. R.A. Fava, "Differential Scanning Calorimetry of Epoxy Resins", Polymer, 9, 137, (1968).
18. K. Horie, H. Hiura, M. Sawada, I. Mita, and H. Kambe, "Calorimetric Investigation of Polymerization Reaction", J. Polym. Sci; Part A-1, Vol. 8, 1357 (1970).
19. M. Cizmecioglu and A. Gupta, "Curing Kinetics of Epoxy Matrix Resins by Differential Scanning Calorimetry", Proceedings of the 37th Annual Technical Conference on Reinforced Plastics/Composites Institute, SPI, 1982, Sec. 20-E.
20. M.R. Kamal and S. Sourour, "Kinetics and Thermal Characterization of Thermoset Cure", Polym. Eng. Sci., 13, 59 (1973).
21. S. Sourour and M.R. Kamal, Thermochim. Acta., 14, 41 (1976).
22. R.B. Prime, "DSC of the Epoxy Cure Reaction", Polym. Eng. Sci., 13, 365 (1973).
23. M.A. Acitelli, R.B. Prime, and E. Sacher, "Kinetics of Epoxy Cure", Polymer, 12, 335 (1971).
24. S.Y. Choy, SPE Journal, 26, 51, (1970).
25. I.T. Smith, "The Mechanism of the Crosslinking of Epoxide Resin by Amines", Polymer, 2, 95 (1961).
26. L.T. Pappalardo, Soc. Plast. Eng. Tech. Papers, 20, 13 (1974).
27. T.A. Dutta, and M.E. Ryan, "Effect of Fillers on Kinetics of Epoxy Cure", J. Appl. Polym. Sci., 24, 635 (1979).
28. B.G. Parker and C.H. Smith, "Evaluating Cure and Shelf Life of Epoxy Prepregs and Film Adhesives", Modern Plastics, 58, Dec. 1979.

29. N.S. Schneider, J.F. Sprouse, G.L. Hagnauer, and J.K. Gillham, "DSC and TBA Studies of the Curing Behavior of Two Dicy-Containing Epoxy Resins", *Polym. Eng. Sci.*, 19, 304, (1979).
30. A.G. Ulukhanov, V.A. Lapitskii, M.S. Akutin, and L.D. Skokova, "Use of DTA for Estimating the Gel-forming Time of Epoxy Binders", *Plast. Massy*, 1981, (9), 59.
31. ASTM D2471-71, "Gel Time and Peak Exothermic Temperature of Reacting Thermosetting Resins", 1970.
32. J.K. Gillham and J.A. Benci, "Isothermal Transitions of a Thermosetting System", *J. Polym. Sci., Symp. No. 46*, 279 (1974).
33. J.K. Gillham, "Characterization of Thermosetting Materials by TBA", *Polym. Eng. Sci.*, 16, 353 (1976).
34. P.G. Babayersky and J.K. Gillham, "Dynamic Mechanical Analysis of the Reactions of Aromatic Diamines with the Diglycidyl Ether of Bisphenol A", *J. Appl. Polym. Sci.*, 17, 2067 (1973).
35. N.S. Schneider and J.K. Gillham, "TBA Studies of Prepreg Curing Behavior", *Polym. Comp.*, 1(2), 97 (1980).
36. G.A. Senich, W.J. Macknight, N.S. Schneider, "A Dynamic Mechanical Study of the Curing Reaction of Two Epoxy Resins", *Polym. Eng. Sci.*, 19, 313 (1979).
37. I.J. Goldfarb and C.Y.C. Lee, "TICA; Thermal Mechanical Behavior of Partially Cured Epoxy Resins", *Am. Chem. Soc. Div. Org. Coat. Plast. Chem.*, 41, 386 (1979).
38. L.E. Neilsen, "Transitions in Polymer Melts", *Polym. Eng. and Sci.*, 17, 713 (1979).
39. C.M. Tung and P.J. Dynes, "Relationship between Viscoelastic Properties and Gelation in Thermosetting Systems", *J. Appl. Polym. Sci.*, 27, 569 (1982).
40. K.E. Reed, "Dynamic Mechanical Analysis of Fiber Reinforced Composites", *Proceedings of the 34th Annual Technical Conference on Reinforced Plastics/Composites Institute, SPI, 1979, Sec. 22-G*.
41. P. Griffiths, "FTIR: Theory and Instrumentation", in Transform Techniques in Chemistry, P. Griffiths, Ed., Plenum Press, 1978, p. 120.
42. J.W. Cooley and J.W. Tukey, *Math. Comput.*, 19, 297 (1965).
43. R. Norton and R. Beer, *J. Opt. Soc. Am.*, 66, 3 (1976).

43. R. Norton and R. Beer, *J. Opt. Soc. Am.*, 66, 3 (1976).
44. J. Chamberlain, "The Principles of Interferometric Spectroscopy, John Wiley & Sons Publ. Co., New York, 1979.
45. J. Rabolt and R. Bellar, "The Nature of Apodization in Fourier Transform Spectroscopy", *Appl. Spect.*, 35, 132 (1981).
46. E.M. Pearce, B.J. Bulkin, S.C. Lin, "Application of Fourier Transform IR to Degradation Studies of Epoxy Systems", *J. Polym. Sci., Polym. Chem. Ed.*, 17, 3121 (1979).
47. M.K. Antoon, Ph.D. Dissertation, Case Western Reserve University, Cleveland, Oh., 1980, Appendix I.
48. J.L. Perkinson, "A Method of Obtaining a True Infrared Spectrum of the Epoxy from a Cured Fiberglass-Epoxy Composite", *Govt. Rep. Announce (U.S.)*, 71(19), 88, 1971.
49. H. Dannenberg, *SPE Trans.*, 78-88 (Jan. 1963).
50. M.K. Antoon and J.L. Koenig, "Crosslinking Mechanism of an Anhydride-Cured Epoxy Resin as Studied by FTIR", *J. Polym. Sci., Polym. Chem. Ed.*, 19, 549 (1981).
51. G.C. Stevens, "Cure Kinetics of Epoxy Resins", *J. Appl. Polym. Sci.*, 26, 4279 (1981).
52. C.A. Byrne, G.L. Hagauer, N.S. Schneider, and R.W. Lenz, "Model Compound Studies on the Amine Cure of Epoxy Resins", *Polym. Comp.*, Dec. 1(2), 71 Dec. 1980.
53. J.F. Sprouse, B.M. Halpin, R.E. Sacher, "Cure Analysis of Epoxy Composites Using FTIR", *Govt. Rept., Announce Index (U.S.)* 79(17), 136, (1979).
54. M.K. Antoon, K.M. Starkey, and J.L. Koenig, "Applications of FTIR to Quality Control of the Epoxy Matrix", *Composite Materials (fifth conference), Testing and Design, ASTM, STP 674*, 541 (1979).
55. M.K. Antoon, B.E. Zehner, and J.L. Koenig, "Spectroscopic Determination of the In-Situ Composition of Epoxy Matrices in Glass Fiber-Reinforced Composites", *Polym. Comp.*, 2(2), 81, April 1981.
56. G.A. George, R.E. Sacher, and J.F. Sprouse, "Photo-oxidation and photoprotection of the Surface Resin of a Glass Fiber-Epoxy Composite", *J. Appl. Polym. Sci.*, 21, 2241 (1977).
57. M.K. Antoon, and J.L. Koenig, "Irreversible Effects of Moisture on the Epoxy Matrix in Glass Fiber-Reinforced Composites", *J. Polym. Sci., Polym. Phys., Ed.*, 19, 197 (1981).

58. C.S. Lu, and J.L. Koenig, "Raman Spectra of Epoxy", Am. Chem. Soc. Div. Org. Coat. Plast. Chem., 32(1), 112 (1972).
59. S.D. Senturia, N.F. Sheppard, S.Y. Poh, and H.R. Appelman, "The Feasibility of Electrical Monitoring of Resin Cure with the Charge Flow Transistor", Polym. Eng. Sci., 21, 112 (1981).
60. J. Chottiner, E.N. Sanjana, M.R. Kodani, K.W. Lengel, G.B. Rosenblatt, "Monitoring Cure of Autoclave-Molded Parts by Dielectric Analysis", Polym. Comp., 13(2), 59, April, 1982.
61. S.M. Ellerstein, "Analytical Calorimetry", R.S. Porter, and J.F. Johnson, Eds., Plenum Press, N.Y., p. 279 (1968).
62. H.J. Borchardt and F. Daniels, "The Application of DSC to the Study of Reaction Kinetics", J. Amer. Chem. Soc., 79, 41 (1957).
63. L.W. Crane, P.J. Dynes and D.H. Kaelble, J. Polym. Sci., Polym. Lett. Ed., 11, 533 (1973).
64. H.E. Kissinger, "Reaction Kinetics in Differential Thermal Analysis", Analy. Chem., 29, 1702 (1957).

15.0 INDEX

absorbance subtraction, 30
accelerators, 3
activation energy, 11, 17
acyclic bisphenol, 5
amine(s), 2,3,4,5,13
anhydride(s), 2,3,35,58
apodization, 26
aramid fiber, 19
Beer-Lambert Law, 28,29,49
B-stage, 4
bisphenol A, 3,5,13,53,55,61
bisphenol S, 5
calorimetric, 8
calorimetry, 1,8
carbon black, 13
carbon fiber, 19
chemical analysis, 53
crosslinking, 5,8,10,20,35,45,46,49,53,61,64
curing, 1,2,3,4,8,10,11,12,13,15,20,22,27,35,45,61,62,64
curve-fitting, 31,46,49
cycloaliphatic epoxide(s), 6
deconvolute, 29
diamine, 4,13
degradation, 3,15,27,32,35,53,55,58,64
dielectric analysis, 1,61,62,64
dielectrometry, 62
diepoxides, 5
diepoxy bisphenols, 5
diepoxy cycloaliphatics, 5
difference spectra, 31,45,53,55
diffuse reflectance, 32,33,34
diluent, 2
dissipation factor, 62
durability, 1
dynamical mechanical, 1,17,20,22
dynamic mechanical test, 1,17,20
DSC, 8,10,11,12,13,15,53,64
DTA, 8,15
epichlorohydrin-bisphenol A, 2
epoxy, 1,2,3,4,5,6,8,10,11,12,13,15,17,19,20,22,27,28,31,32,33,
34,35,45,46,49,53,55,58,61,62,64
epoxy novolak, 2
factor, 2,10,13,17,25,27,28,29,30,31,32,46,49,62
factor analysis, 28,29
Fourier transform spectroscopy, 23
FT-IR, 22,24,27,28,31,32,33,34,45
gas chromatography, 53
glycidyl amine(s), 5

continued...

Index continued...

glycidyl esters, 5
heat-deflection-temperature 5,6
heat resistance, 5
impact strength, 2,6
infrared spectroscopy, 22,23,35,53
interferometer, 23,25
internal reflectance, 46,53
internal-reflection, 33
least-square(s), 30,31,49,53
loss factor, 62
mass spectroscopy, 53
multiple internal reflection (MIR), 33
nadic methyl anhydride, 35
near-IR, 28,35,45
novolac(s), 5,55
novolac epoxy, 53,55
photo-oxidation, 53,55
polyimides, 5
polyolefin, 2
prepregs, 4,13
quality control, 28,46
Raman, 28,34,58
Raman spectroscopy, 58
reliability, 1,46
reproducibility, 1,28
S-glass, 59,53
shelf-life, 4,13
silica(s), 13,44
spectroscopy, 1,22,23,25,32,35,45,53,58,61,64
TBA, 17,19,20,64
tetraglycidyl methylenedianiline, 15
torsional braid analysis, 17,19
transmission spectroscopy, 32
visco-elastic tester, 19
viscosity, 2,3,17,20
weathering, 28,53,55

DISTRIBUTION LIST

No. of Copies	To
	Commander, U.S. Army Aviation Research and Development Command, 4300 Goodfellow Boulevard, St. Louis, MO 63120
10	ATTN: DRDAV-EGX
1	DRDAV-D
1	DRDAV-N
	Project Manager, Advanced Attack Helicopter, 4300 Goodfellow Boulevard, St. Louis, MO 63120
2	ATTN: DRCPM-AAH-TM
1	DRCPM-AAH-TP
	Project Manager, Black Hawk, 4300 Goodfellow Boulevard, St. Louis, MO 63120
2	ATTN: DRCPM-BH-T
	Project Manager, CH-47 Modernization, 4300 Goodfellow Boulevard, St. Louis, MO 63166
2	ATTN: DRCPM-CH-47-MT
	Project Manager, Aircraft Survivability Equipment, 4300 Goodfellow Boulevard, St. Louis, MO 63120
2	ATTN: DRCPM-ASE-TM
	Project Manager, Cobra, 4300 Goodfellow Boulevard, St. Louis, MO 63120
2	ATTN: DRCPM-CO-T
	Project Manager, Advanced Scout Helicopter, 4300 Goodfellow Boulevard, St. Louis, MO 63120
2	ATTN: DRCPM-ASH
	Project Manager, Tactical Airborne Remotely Piloted Vehicle/Drone Systems, 4300 Goodfellow Boulevard, St. Louis, MO 63120
2	ATTN: DRCPM-RPV
	Project Manager, Navigation/Control Systems, Fort Monmouth, NJ 07703
2	ATTN: DRCPM-NC-TM
	Commander, U.S. Army Materiel Development and Readiness Command, 5001 Eisenhower Avenue, Alexandria, VA 22333
4	ATTN: DRCMT
2	DRCPM
	Director, Applied Technology Laboratory, Research and Technology Laboratories (AVRADCOM), Fort Eustis, VA 23604
2	ATTN: DAVDL-ATL-ATS
	Director, Research and Technology Laboratories (AVRADCOM), Moffett Field, CA 94035
2	ATTN: DAVDL-AL-D

No. of
Copies

To

-
- Headquarters, Naval Sea Systems Command, 1941 Jefferson Davis Highway,
Arlington, VA 22376
1 ATTN: Code 035
- Headquarters, Naval Electronics Systems Command, Washington, D.C. 20360
1 ATTN: Code 504
- Director, Naval Material Command, Industrial Resources Detachment, Building 75-2,
Naval Base, Philadelphia, PA 19112
1 ATTN: Technical Director
- Commander, U.S. Air Force Wright Aeronautical Laboratories, Wright-Patterson
Air Force Base, OH 45433
1 ATTN: AFWAL/MLTN
1 AFWAL/MLTM
1 AFWAL/MLTE
1 AFWAL/MLTC
- National Aeronautics and Space Administration, Washington, D.C. 20546
1 ATTN: AFSS-AD, Office of Scientific and Technical Document Information
- National Aeronautics and Space Administration, Marshall Space Flight Center,
Huntsville, AL 35812
1 ATTN: R. J. Schwinghammer, EH01, Dir., M&P Lab
1 Mr. W. A. Wilson, EH41, Bldg 4612
- 2 Metals and Ceramics Information Center, Battelle Columbus Laboratories,
505 King Avenue, Columbus, OH 43201
- Hughes Helicopters-Summa, M/S T-419, Centinella Avenue and Teale Street,
Culver City, CA 90230
2 ATTN: Mr. R. E. Moore, Bldg. 314
- Sikorsky Aircraft Division, United Aircraft Corporation, Stratford, CT 06497
2 ATTN: Mr. Melvin M. Schwartz, Chief, Manufacturing Technology
- Bell Helicopter Textron, Division of Textron, Inc., P.O. Box 482,
Fort Worth, TX 76101
2 ATTN: Mr. P. Baumgartner, Chief, Manufacturing Technology
- Kaman Aerospace Corporation, Bloomfield, CT 06002
2 ATTN: Mr. A. S. Falcone, Chief, Materials Engineering
- Boeing Vertol Company, Box 16858, Philadelphia, PA 19142
2 ATTN: R. Pinckney, Manufacturing Technology
2 R. Drago, Advanced Drive Systems Technology
- Detroit Diesel Allison Division, General Motors Corporation, P.O. Box 894,
Indianapolis, IN 46206
2 ATTN: James E. Knott, General Manager

No. of
Copies

To

1 Commander, U.S. Army Armament Research and Development Command, Dover, NJ 07801
1 ATTN: DRDAR-PML
1 Technical Library
1 Mr. Harry E. Pebly, Jr., PLASTECH, Director

1 Commander, U.S. Army Armament Research and Development Command,
Watervliet, NY 12189
1 ATTN: DRDAR-LCB-S
1 SARWV-PPI

1 Commander, U.S. Army Armament Materiel Readiness Command, Rock Island, IL 61299
1 ATTN: DRSAR-IRB
1 DRSAR-IMC
1 Technical Library

1 Commander, U.S. Army Foreign Science and Technology Center, 220 7th Street, N.E.,
Charlottesville, VA 22901
1 ATTN: DRXST-SD3

1 Commander, U.S. Army Electronics Research and Development Command,
Fort Monmouth, NJ 07703
1 ATTN: DELET-DS

1 Commander, U.S. Army Electronics Research and Development Command,
2800 Powder Mill Road, Adelphi, MD 20783
1 ATTN: DRDEL-BC

1 Commander, U.S. Army Depot Systems Command, Chambersburg, PA 17201
1 ATTN: DRSDS-PMI

1 Commander, U.S. Army Test and Evaluation Command, Aberdeen Proving
Ground, MD 21005
1 ATTN: DRSTE-ME

1 Commander, U.S. Army Communications-Electronics Command,
Fort Monmouth, NJ 07703
1 ATTN: DRSEL-LE-R
1 DRSEL-POD-P

1 Director, U.S. Army Ballistic Research Laboratory, Aberdeen Proving Ground,
MD 21005
1 ATTN: DRDAR-TSB-S (STINFO)

1 Chief of Naval Research, Arlington, VA 22217
1 ATTN: Code 472

1 Headquarters, Naval Material Command, Washington, D.C. 20360
1 ATTN: Code MAT-042M

1 Headquarters, Naval Air Systems Command, Washington, D.C. 20361
1 ATTN: Code 5203

No. of
Copies

To

Director, Langley Directorate, U.S. Army Air Mobility Research and Development
Laboratories (AVRADCOM), Hampton, VA 23365
2 ATTN: DAVDL-LA, Mail Stop 266

Commander, U.S. Army Avionics Research and Development Activity,
Fort Monmouth, NJ 07703
2 ATTN: DAVAA-O

Director, Lewis Directorate, U.S. Army Air Mobility Research and Development
Laboratories, 21000 Brookpark Road, Cleveland, OH 44135
2 ATTN: DAVDL-LE

Director, U.S. Army Industrial Base Engineering Activity, Rock Island Arsenal,
Rock Island, IL 61299
4 ATTN: DRXIB-MT

Commander, U.S. Army Troop Support and Aviation Materiel Readiness Command,
4300 Goodfellow Boulevard, St. Louis, MO 63120
1 ATTN: DRSTS-PLC
1 DRSTS-ME
2 DRSTS-DIL

Office of the Under Secretary of Defense for Research and Engineering,
The Pentagon, Washington, D.C. 20301
1 ATTN: Dr. L. L. Lehn, Room 3D 1079

12 Commander, Defense Technical Information Center, Cameron Station,
Alexandria, VA 22314

Headquarters, Department of the Army, Washington, D.C. 20301
2 ATTN: DAMA-CSS, Dr. J. Bryant
1 DAMA-PPP, Mr. R. Vawter
1 DUSRDE(AM), Mr. R. Donnelly

Director, Defense Advanced Research Projects Agency, 1400 Wilson Boulevard,
Arlington, VA 22209
1 ATTN: Dr. A. Bement

Commander, U.S. Army Missile Command, Redstone Arsenal, AL 35809
1 ATTN: DRSMI-ET
1 DRSMI-RBLD, Redstone Scientific Information Center
1 DRSMI-NSS

Commander, U.S. Army Tank-Automotive Command, Warren, MI 48090
1 ATTN: DRSTA-R
1 DRSTA-RCKM
1 Technical Library
1 DRSTA-EB

No. of Copies	To
2	General Electric Company, 10449 St. Charles Rock Road, St. Ann, MO 63074 ATTN: Mr. H. Franzen
2	AVCO-Lycoming Corporation, 550 South Main Street, Stratford, CT 08497 ATTN: Mr. V. Strautman, Manager, Process Technology Laboratory
2	United Technologies Corporation, Pratt & Whitney Aircraft Division, Manufacturing Research and Development, East Hartford, CT 06108 ATTN: Mr. Ray Traynor
2	Grumman Aerospace Corporation, Plant 2, Bethpage, NY 11714 ATTN: Richard Cyphers, Manager, Manufacturing Technology Albert Greci, Manufacturing Engineer, Department 231
2	Lockheed Missiles and Space Company, Inc., Manufacturing Research, 1111 Lockheed Way, Sunnyvale, CA 94088 ATTN: H. Dorfman, Research Specialist
2	Lockheed Missiles and Space Company, Inc., P.O. Box 504, Sunnyvale, CA 94086 ATTN: D. M. Schwartz, Dept. 55-10, Bldg. 572
1	Mr. R. J. Zentner, EAI Corporation, 198 Thomas Johnson Drive, Suite 16, Frederick, MD 21701
2	Director, Army Materials and Mechanics Research Center, Watertown, MA 02172
1	ATTN: DRXMR-PL
1	DRXMR-PR
1	DRXMR-K
1	DRXMR-FD
10	DRXMR-OC, Dr. Richard Shuford

U.S. Army Aviation Research and Development Command,
Attn: DRDAV-EGX, St. Louis, MO. 63120
Quality Control and Nondestructive Evaluation
Techniques for Composites - Part II: Physio-
chemical Characterization Techniques - A State-
of-the-art Review - Jack L. Koenig, Case West-
ern Reserve University, Cleveland, Oh., 44106

Technical Report AVRADCOM TR 83-F-6 (AMMRC TR 83-24),
May 1983, illus-tables, Contract DAAG29-81-D-D100
D/A Project 1827119, AMCMS Code 1497.2D, Agency
Accession: DDS7119(EF2), Final Report, August
1982 - July 1983.

The physical, chemical, and ultimate mechanical properties of high performance glass fiber-reinforced composites are dependent on the degree of cure and structure of epoxy matrices. Therefore, a knowledge of the curing process and composition of epoxy matrices is essential for relating the properties of composites to the extent of the reaction and optimizing the performance. Several methods have been developed to characterize and control the curing of epoxy matrices. These methods include spectroscopy, differential scanning calorimetry, dielectric analysis, and dynamical mechanical tests. These methods can be used to characterize the curing process during or after the fabrication of the cured epoxy matrices to justify reproducibility, reliability, and durability. In general, a combination of these methods are powerful techniques to analyze and control the quality of epoxy matrices in fiber-reinforced composites. The sensitivity, advantages, and selectivity of these techniques will be reviewed and discussed in this report.

AD

Unclassified
Unlimited Distribution

Key Words

Composite materials
Quality assurance
Quality control
Epoxy Resins
Infrared spectroscopy
Fiber-reinforced composites
Curing
State-of-the-art

U.S. Army Aviation Research and Development Command,
Attn: DRDAV-EGX, St. Louis, MO. 63120
Quality Control and Nondestructive Evaluation
Techniques for Composites - Part II: Physio-
chemical Characterization Techniques - A State-
of-the-art Review - Jack L. Koenig, Case West-
ern Reserve University, Cleveland, Oh., 44106

Technical Report AVRADCOM TR 83-F-6 (AMMRC TR 83-24),
May 1983, illus-tables, Contract DAAG29-81-D-D100
D/A Project 1827119, AMCMS Code 1497.2D, Agency
Accession: DDS7119(EF2), Final Report, August
1982 - July 1983.

The physical, chemical, and ultimate mechanical properties of high performance glass fiber-reinforced composites are dependent on the degree of cure and structure of epoxy matrices. Therefore, a knowledge of the curing process and composition of epoxy matrices is essential for relating the properties of composites to the extent of the reaction and optimizing the performance. Several methods have been developed to characterize and control the curing of epoxy matrices. These methods include spectroscopy, differential scanning calorimetry, dielectric analysis, and dynamical mechanical tests. These methods can be used to characterize the curing process during or after the fabrication of the cured epoxy matrices to justify reproducibility, reliability, and durability. In general, a combination of these methods are powerful techniques to analyze and control the quality of epoxy matrices in fiber-reinforced composites. The sensitivity, advantages, and selectivity of these techniques will be reviewed and discussed in this report.

AD

Unclassified
Unlimited Distribution

Key Words

Composite materials
Quality assurance
Quality control
Epoxy Resins
Infrared spectroscopy
Fiber-reinforced composites
Curing
State-of-the-art

U.S. Army Aviation Research and Development Command,
Attn: DRDAV-EGX, St. Louis, MO. 63120
Quality Control and Nondestructive Evaluation
Techniques for Composites - Part II: Physio-
chemical Characterization Techniques - A State-
of-the-art Review - Jack L. Koenig, Case West-
ern Reserve University, Cleveland, Oh., 44106

Technical Report AVRADCOM TR 83-F-6 (AMMRC TR 83-24),
May 1983, illus-tables, Contract DAAG29-81-D-D100
D/A Project 1827119, AMCMS Code 1497.2D, Agency
Accession: DDS7119(EF2), Final Report, August
1982 - July 1983.

The physical, chemical, and ultimate mechanical properties of high performance glass fiber-reinforced composites are dependent on the degree of cure and structure of epoxy matrices. Therefore, a knowledge of the curing process and composition of epoxy matrices is essential for relating the properties of composites to the extent of the reaction and optimizing the performance. Several methods have been developed to characterize and control the curing of epoxy matrices. These methods include spectroscopy, differential scanning calorimetry, dielectric analysis, and dynamical mechanical tests. These methods can be used to characterize the curing process during or after the fabrication of the cured epoxy matrices to justify reproducibility, reliability, and durability. In general, a combination of these methods are powerful techniques to analyze and control the quality of epoxy matrices in fiber-reinforced composites. The sensitivity, advantages, and selectivity of these techniques will be reviewed and discussed in this report.

AD

Unclassified
Unlimited Distribution

Key Words

Composite materials
Quality assurance
Quality control
Epoxy Resins
Infrared spectroscopy
Fiber-reinforced composites
Curing
State-of-the-art

U.S. Army Aviation Research and Development Command,
Attn: DRDAV-EGX, St. Louis, MO. 63120
Quality Control and Nondestructive Evaluation
Techniques for Composites - Part II: Physio-
chemical Characterization Techniques - A State-
of-the-art Review - Jack L. Koenig, Case West-
ern Reserve University, Cleveland, Oh., 44106

Technical Report AVRADCOM TR 83-F-6 (AMMRC TR 83-24),
May 1983, illus-tables, Contract DAAG29-81-D-D100
D/A Project 1827119, AMCMS Code 1497.2D, Agency
Accession: DDS7119(EF2), Final Report, August
1982 - July 1983.

The physical, chemical, and ultimate mechanical properties of high performance glass fiber-reinforced composites are dependent on the degree of cure and structure of epoxy matrices. Therefore, a knowledge of the curing process and composition of epoxy matrices is essential for relating the properties of composites to the extent of the reaction and optimizing the performance. Several methods have been developed to characterize and control the curing of epoxy matrices. These methods include spectroscopy, differential scanning calorimetry, dielectric analysis, and dynamical mechanical tests. These methods can be used to characterize the curing process during or after the fabrication of the cured epoxy matrices to justify reproducibility, reliability, and durability. In general, a combination of these methods are powerful techniques to analyze and control the quality of epoxy matrices in fiber-reinforced composites. The sensitivity, advantages, and selectivity of these techniques will be reviewed and discussed in this report.

AD

Unclassified
Unlimited Distribution

Key Words

Composite materials
Quality assurance
Quality control
Epoxy Resins
Infrared spectroscopy
Fiber-reinforced composites
Curing
State-of-the-art

U.S. Army Aviation Research and Development Command,
Attn: DRDAV-EGX, St. Louis, MO. 63120
Quality Control and Nondestructive Evaluation
Techniques for Composites - Part II: Physio-
chemical Characterization Techniques - A State-
of-the-art Review - Jack L. Koenig, Case West-
ern Reserve University, Cleveland, Oh., 44106

Technical Report AVRADCOM TR 83-F-5 (AMMRC TR 83-74),
May 1983, 111us-tables, Contract DAAG29-81-D-D100
D/A Project 1827119, AMMS Code 1497.2D, Agency
Accession: DDS7119(EF2), Final Report, August
1982 - July 1983.

The physical, chemical, and ultimate mechanical properties of high performance glass fiber-reinforced composites are dependent on the degree of cure and structure of epoxy matrices. Therefore, a knowledge of the curing process and composition of epoxy matrices is essential for relating the properties of composites to the extent of the reaction and optimizing the performance. Several methods have been developed to characterize and control the curing of epoxy matrices. These methods include spectroscopy, differential scanning calorimetry, dielectric analysis, and dynamical mechanical tests. These methods can be used to characterize the curing process during or after the fabrication of the cured epoxy matrices to justify reproducibility, reliability, and durability. In general, a combination of these methods are powerful techniques to analyze and control the quality of epoxy matrices in fiber-reinforced composites. The sensitivity, advantages, and selectivity of these techniques will be reviewed and discussed in this report.

AD
Unclassified
Unlimited Distribution

Key Words
Composite materials
Quality assurance
Quality control
Epoxy Resins
Infrared spectroscopy
Fiber-reinforced composites
Curing
State-of-the-art

U.S. Army Aviation Research and Development Command,
Attn: DRDAV-EGX, St. Louis, MO. 63120
Quality Control and Nondestructive Evaluation
Techniques for Composites - Part II: Physio-
chemical Characterization Techniques - A State-
of-the-art Review - Jack L. Koenig, Case West-
ern Reserve University, Cleveland, Oh., 44106

Technical Report AVRADCOM TR 83-F-6 (AMMRC TR 83-74),
May 1983, 111us-tables, Contract DAAG29-81-D-D100
D/A Project 1827119, AMMS Code 1497.2D, Agency
Accession: DDS7119(EF2), Final Report, August
1982 - July 1983.

The physical, chemical, and ultimate mechanical properties of high performance glass fiber-reinforced composites are dependent on the degree of cure and structure of epoxy matrices. Therefore, a knowledge of the curing process and composition of epoxy matrices is essential for relating the properties of composites to the extent of the reaction and optimizing the performance. Several methods have been developed to characterize and control the curing of epoxy matrices. These methods include spectroscopy, differential scanning calorimetry, dielectric analysis, and dynamical mechanical tests. These methods can be used to characterize the curing process during or after the fabrication of the cured epoxy matrices to justify reproducibility, reliability, and durability. In general, a combination of these methods are powerful techniques to analyze and control the quality of epoxy matrices in fiber-reinforced composites. The sensitivity, advantages, and selectivity of these techniques will be reviewed and discussed in this report.

AD
Unclassified
Unlimited Distribution

Key Words
Composite materials
Quality assurance
Quality control
Epoxy Resins
Infrared spectroscopy
Fiber-reinforced composites
Curing
State-of-the-art

U.S. Army Aviation Research and Development Command,
Attn: DRDAV-EGX, St. Louis, MO. 63120
Quality Control and Nondestructive Evaluation
Techniques for Composites - Part II: Physio-
chemical Characterization Techniques - A State-
of-the-art Review - Jack L. Koenig, Case West-
ern Reserve University, Cleveland, Oh., 44106

Technical Report AVRADCOM TR 83-F-6 (AMMRC TR 83-74),
May 1983, 111us-tables, Contract DAAG29-81-D-D100
D/A Project 1827119, AMMS Code 1497.2D, Agency
Accession: DDS7119(EF2), Final Report, August
1982 - July 1983.

The physical, chemical, and ultimate mechanical properties of high performance glass fiber-reinforced composites are dependent on the degree of cure and structure of epoxy matrices. Therefore, a knowledge of the curing process and composition of epoxy matrices is essential for relating the properties of composites to the extent of the reaction and optimizing the performance. Several methods have been developed to characterize and control the curing of epoxy matrices. These methods include spectroscopy, differential scanning calorimetry, dielectric analysis, and dynamical mechanical tests. These methods can be used to characterize the curing process during or after the fabrication of the cured epoxy matrices to justify reproducibility, reliability, and durability. In general, a combination of these methods are powerful techniques to analyze and control the quality of epoxy matrices in fiber-reinforced composites. The sensitivity, advantages, and selectivity of these techniques will be reviewed and discussed in this report.

AD
Unclassified
Unlimited Distribution

Key Words
Composite materials
Quality assurance
Quality control
Epoxy Resins
Infrared spectroscopy
Fiber-reinforced composites
Curing
State-of-the-art

U.S. Army Aviation Research and Development Command,
Attn: DRDAV-EGX, St. Louis, MO. 63120
Quality Control and Nondestructive Evaluation
Techniques for Composites - Part II: Physio-
chemical Characterization Techniques - A State-
of-the-art Review - Jack L. Koenig, Case West-
ern Reserve University, Cleveland, Oh., 44106

Technical Report AVRADCOM TR 83-F-6 (AMMRC TR 83-74),
May 1983, 111us-tables, Contract DAAG29-81-D-D100
D/A Project 1827119, AMMS Code 1497.2D, Agency
Accession: DDS7119(EF2), Final Report, August
1982 - July 1983.

The physical, chemical, and ultimate mechanical properties of high performance glass fiber-reinforced composites are dependent on the degree of cure and structure of epoxy matrices. Therefore, a knowledge of the curing process and composition of epoxy matrices is essential for relating the properties of composites to the extent of the reaction and optimizing the performance. Several methods have been developed to characterize and control the curing of epoxy matrices. These methods include spectroscopy, differential scanning calorimetry, dielectric analysis, and dynamical mechanical tests. These methods can be used to characterize the curing process during or after the fabrication of the cured epoxy matrices to justify reproducibility, reliability, and durability. In general, a combination of these methods are powerful techniques to analyze and control the quality of epoxy matrices in fiber-reinforced composites. The sensitivity, advantages, and selectivity of these techniques will be reviewed and discussed in this report.

AD
Unclassified
Unlimited Distribution

Key Words
Composite materials
Quality assurance
Quality control
Epoxy Resins
Infrared spectroscopy
Fiber-reinforced composites
Curing
State-of-the-art

R



60467